Atmospheric
Chemistry
and Physics

Open Access

Research article

Fine-scale fluctuations of PM$_1$, PM$_{2.5}$, PM$_{10}$ and SO$_2$ concentrations caused by a prolonged volcanic eruption (Fagradalsfjall 2021, Iceland)

Rachel C. W. Whitty[1], **Evgenia Ilyinskaya**[1], **Melissa A. Pfeffer**[2], **Ragnar H. Thrastarson**[2],
Þorsteinn Johannsson[3], **Sara Barsotti**[2], **Tjarda J. Roberts**[4,5], **Guðni M. Gilbert**[2,6], **Tryggvi Hjörvar**[2],
Anja Schmidt[7,8,9], **Daniela Fecht**[10], and **Grétar G. Sæmundsson**[11]

[1]COMET, Institute of Geophysics and Tectonics, School of Earth and Environment,
University of Leeds, Leeds, LS2 9JT, United Kingdom
[2]Icelandic Meteorological Office, 150 Reykjavík, Iceland
[3]The Environment Agency of Iceland, 108 Reykjavík, Iceland
[4]CNRS UMR7328, Laboratoire de Physique et de Chimie de l'Environnement et de l'Espace,
Universite d'Orleans, 45071 Orleans, France
[5]LMD/IPSL, ENS, Université PSL, École Polytechnique, Institute Polytechnique de Paris,
Sorbonne Université, CNRS, 75005 Paris, France
[6]Nox Medical, 150 Reykjavík, Iceland
[7]Yusuf Hamed Department of Chemistry, University of Cambridge, Cambridge, CB2 1EW, United Kingdom
[8]Institute of Atmospheric Physics (IPA), German Aerospace Centre (DLR), 82234 Oberpfaffenhofen, Germany
[9]Meteorological Institute, Ludwig Maximilian University of Munich, 80333 Munich, Germany
[10]MRC Centre for Environment and Health, School of Public Health,
Imperial College London, London, W12 0BZ, United Kingdom
[11]Department of Research and Analysis, Icelandic Tourist Board, 101 Reykjavík, Iceland

Correspondence: Evgenia Ilyinskaya (e.ilyinskaya@leeds.ac.uk)

Abstract. The 2021 Fagradalsfjall eruption marked the first in a series of ongoing eruptions in a densely populated region of Iceland ($> 260\,000$ residents within 50 km distance). This eruption was monitored by an exceptionally dense regulatory air quality network, providing a unique opportunity to examine fine-scale dispersion patterns of volcanic air pollutants (SO$_2$, PM$_1$, PM$_{2.5}$, PM$_{10}$) in populated areas.

Despite its relatively small size, the eruption led to statistically-significant increases in PM and SO$_2$ concentrations at distances of at least 300 km. Peak daily-mean concentrations of PM$_1$ (measured in the capital area, 25–35 km distance from the source) rose from 5–6 to 18–20 µg m^{-3}, and the proportion of PM$_1$ within PM$_{10}$ increased by $\sim 50\,\%$. In areas with low background pollution, average PM$_{10}$ and PM$_{2.5}$ levels increased by $\sim 50\,\%$ but in places with high background sources, the eruption's impact was not detectable. These findings suggest that ash-poor eruptions are a major source of PM$_1$ in Iceland and potentially in other regions exposed to volcanic emissions.

Air quality guidelines for PM$_1$ and SO$_2$ were exceeded more frequently during the eruption than under background conditions. This suggests the potential for an increase in adverse health effects. Moreover, pollutant concentrations exhibited strong fine-scale temporal (≤ 1 h) and spatial (< 1 km) variability. This suggests disparities in population exposures to volcanic air pollution, even from relatively distal sources, and underscores the importance of a dense monitoring network and effective public communication.

1   Introduction

Airborne volcanic emissions pose both acute and chronic health hazards that can affect populations across large geographic areas (Stewart et al., 2021, and references within). Globally, over one billion people are estimated to live within 100 km of an active volcano (Freire et al., 2019), a distance within which they might be exposed to volcanic air pollution (Stewart et al., 2021). The number of potentially exposed people is growing, for example, due to building expansion into previously uninhabited areas near volcanoes. In this study, we examine the impacts of volcanic emissions on air quality in populated areas using high-resolution, high-quality observational data. We focus on the 2021 Fagradalsfjall fissure eruption on the Reykjanes peninsula as a case study. Fissure eruptions are one of the most common types of volcanic activity that affects air quality. Recent examples include the Kīlauea volcano in Hawai'i (with tens of episodes since 1983), Cumbre Vieja on La Palma in 2021, and the Reykjanes peninsula in Iceland (11 eruptions since 2021). Fissure eruptions have low explosivity and produce negligible ash but release prodigious amounts of gases and aerosol particulate matter close to ground level. Even small fissure eruptions can cause severe air pollution episodes (Whitty et al., 2020).

Fine-scale spatial variability in air pollutant concentrations – characterized by steep gradients over distances of just a few kilometres or less – is currently one of the most active areas of research within the broader field of air pollution (Apte and Manchanda, 2024). In urban areas, these fine-scale variations contribute to disparities in air quality, population exposure, and associated physical, mental, and social well-being (Apte and Manchanda, 2024, and references within). The 2021 Fagradalsfjall eruption provided a novel opportunity to investigate the fine-scale variability of volcanic air pollution in urban settings, as it was monitored by an exceptionally dense regulatory air quality network. Here, we use the term "regulatory" to describe an air quality monitoring network operated by a national agency, employing certified commercial instrumentation with regulated setup and calibration protocols. These networks provide high-accuracy, high-precision measurements with high temporal resolution, but typically with low spatial resolution due to the high costs of installation (typically > EUR 100 000) and maintenance (typically > EUR 100 000 per annum). For example, Germany has approximately one regulatory station per ∼ 250 000 people, with a similar density in the United States (Apte and Manchanda, 2024). In many volcanic regions, regulatory air quality monitoring is either absent or very sparse (Felton et al., 2019). Prior to our study, the best-observed case studies of volcanic air pollution came from Kīlauea volcano in Hawaii (in particular, its large fissure eruption in 2018), and the large Holuhraun fissure eruption

2014–2015 in Iceland (Crawford et al., 2021; Gíslason et al., 2015; Ilyinskaya et al., 2017; Schmidt et al., 2015; Whitty et al., 2020). These events were monitored by relatively few and distant regulatory stations – approximately 90 km from the eruption site at Holuhraun and about 40 km at Kīlauea. In contrast, the 2021 Fagradalsfjall eruption occurred in Iceland's most densely populated region and in response, national authorities made a strategic decision early on to expand the regulatory network, ensuring that nearly every community was covered by at least one station. During the eruption, 27 regulatory stations were operational across Iceland, with 14 located within 40 km of the eruption site. Some stations were positioned less than 1 km apart, enabling unprecedented spatial resolution in observing volcanic air pollution.

Regulatory air quality networks can be supplemented by so-called lower-cost sensors (LCS), which are typically small in size (a few centimetres) and cost approximately EUR 200. An active body of research on the expanding use of LCS highlights their potential to enhance the relatively sparse regulatory networks (reviewed in Apte and Manchanda, 2024; and Sokhi et al., 2022). For example, during a two-week campaign in 2018, the regulatory air quality network on Hawai'i Island was augmented with 16 LCS. This denser network significantly changed the estimates of population exposure to volcanic air pollution (Crawford et al., 2021). Despite their advantages in affordability and portability, LCS have notable limitations, including relatively poor accuracy and precision compared to regulatory-grade instruments, and a lack of standardised protocols for installation and maintenance. In our study, LCS were deployed to establish a rapid-response monitoring network directly at the eruption site, aimed at mitigating exposure hazards for the approximately 300 000 visitors who came to view the eruption. We present and discuss the use of LCS in a crisis mitigation context, which has broader relevance for other high-concentration, rapid-onset air pollution events, such as wildfires.

1.1   Volcanic air pollutants and associated health impacts

Much of the existing knowledge on the health impacts of volcanic gases and aerosols comes from epidemiological and public health investigations of the eruptions at Holuhraun in Iceland and Kīlauea in Hawaii. The Holuhraun eruption was associated with increased healthcare utilisation for respiratory conditions in the country's capital area, located approximately 250 km from the eruption site (Carlsen et al., 2021a, b). These findings are consistent with observations from Kīlauea on Hawaii, which have been based on more qualitative health assessments and questionnaire-based surveys (Horwell et al., 2023; Longo, 2009; Longo et al., 2008; Tam et al., 2016). Volcanic emissions contain a wide array of chemical species, many of which are hazardous to human health (Stewart et al., 2021). In this study, we focus on sul-

fur dioxide gas (SO_2) and three particulate matter (PM) size fractions – PM_1, $PM_{2.5}$, PM_{10} – which refer to particles with aerodynamic diameters less than 1, 2.5, and 10 µm, respectively. These pollutants are typically elevated both near the eruption source and at considerable distances downwind reviewed in Stewart et al. (2021). Throughout this work, we use the term "volcanic emissions" to refer collectively to SO_2 and PM, unless otherwise specified.

Sulfur dioxide is abundant in volcanic emissions and a key air pollutant in volcanic areas (Crawford et al., 2021; Gíslason et al., 2015; Ilyinskaya et al., 2017; Schmidt et al., 2015; Whitty et al., 2020). Laboratory studies have shown that individuals with asthma are particularly sensitive to even relatively low concentrations of SO_2 (below $500\,\mu g\,m^{-3}$), and air quality thresholds are typically established to protect this vulnerable group (US EPA National Center for Environmental Assessment, 2008). Epidemiological studies in volcanic regions further indicate that young children (defined as ≤ 4 years old) and the elderly (≥ 64 years old) are more susceptible to adverse health effects from above-threshold SO_2 exposure compared to the general adult population (Carlsen et al., 2021b). This study provides an unprecedented spatial resolution of SO_2 exposure in a densely populated, modern society affected by this pollutant. In recent decades, the number of regulatory air quality stations monitoring SO_2 has declined across much of the Global North, largely due to reductions in anthropogenic emissions, particularly from coal combustion. To our knowledge, Iceland currently maintains the highest number and spatial density of regulatory SO_2 monitoring stations worldwide.

Volcanic emissions are extremely rich in PM, comprising both primary particles emitted directly from the source (including ash) and secondary particles formed through post-emission processes, such as sulfur gas-to-particle conversion. Some eruptions (e.g. at Kīlauea, Cumbre Vieja, and several recent Reykjanes episodes) ignite significant wildfires, which are also a source of PM. All three PM size fractions reported in this study – PM_1, $PM_{2.5}$, PM_{10} – are known to be significantly elevated near volcanic sources. In fissure eruptions, PM_1 is typically the dominant size fraction at-source (Ilyinskaya et al., 2012, 2017; Mather et al., 2003). Exposure to PM air pollution, from natural and anthropogenic sources, has been linked to a wide range of adverse health outcomes, including cardiovascular and respiratory diseases, and lung cancer (Brauer et al., 2024, and references within). Health impacts have been observed even at low concentrations, with children and the elderly particularly vulnerable. The size of PM plays a critical role in determining health impacts. $PM_{2.5}$ has long been associated with worse health outcomes compared to PM_{10} (Janssen et al., 2013; Mcdonnell et al., 2000), and the importance of PM_1 is now a key focus in air pollution and health research. Multiple epidemiological studies from China have found PM_1 exposure to be more strongly correlated with negative health outcomes than $PM_{2.5}$ (Gan et al., 2025; Guo et al., 2022; Yang et al., 2018; Zhang et al.,

2020). In Europe, epidemiological research on PM_1 health impacts is still in its early stages (Tomášková et al., 2024), largely due to a lack of high-quality observational data on PM_1 concentrations and exposure. This study reports on the first three years of regulatory-grade PM_1 measurements in Iceland (2020–2022) and represents the first regulatory-grade time series of PM_1 from a volcanic source.

In volcanic emissions, concentrations of both SO_2 and PM in various size fractions are consistently elevated, but their relative proportions vary depending on several factors, including distance from the source, plume age, and the rate of gas-to-particle conversion. Existing evidence suggests that this variability in plume composition may influence the associated health outcomes in distinct ways. An epidemiological study in Iceland comparing SO_2-dominated plumes with PM-dominated plumes found that the latter was associated with a greater increase in the dispensation of asthma medication and reported cases of respiratory infections (Carlsen et al., 2021a). In contrast, statistically significant increases in healthcare utilization for chronic obstructive pulmonary disease (COPD) were observed only in association with exposure to SO_2-dominated plumes (Carlsen et al., 2021a).

Our study contributes a dataset on different types of volcanic air pollutants with a higher spatial resolution than has previously been possible. This offers a foundation for future epidemiological research into the health impacts of recent and ongoing eruptions in Iceland.

1.2 Fagradalsfjall 2021 eruption

The 2021 Fagradalsfjall event (19 March–19 September 2021) was the first volcanic eruption on the Reykjanes peninsula in nearly 800 years. This region is the most densely populated area of Iceland, with over 260 000 people – around 70 % of the national population – residing within 50 km of the eruption site. The eruption site was 9 km from the town of Grindavík and approximately 25 km from the capital area of Reykjavík (Fig. 1). Although the eruption took place in an uninhabited area, it attracted an estimated 300 000 visitors who observed the event at close range.

The eruption was a basaltic fissure eruption with an effusive and mildly explosive style, dominated by lava fountaining and lava flows (Barsotti et al., 2023). While relatively small in size – emitting a total of ~ 0.3–$0.9\,Mt$ of SO_2 and covering an area of $4.82\,km^2$ with lava (Barsotti et al., 2023; Pfeffer et al., 2024) – its proximity to urban areas and the high number of visitors likely resulted in greater population exposure to volcanic air pollution than any previous eruption in Iceland.

This eruption is considered to mark the onset of a new period of frequent eruptions on the Reykjanes peninsula. Such periods, locally referred to as the "Reykjanes Fires", have occurred roughly every 1000 years, each lasting for decades to centuries. The last period of Reykjanes Fires ended with an eruption in 1240 CE (Sigurgeirsson and Einarsson, 2019).
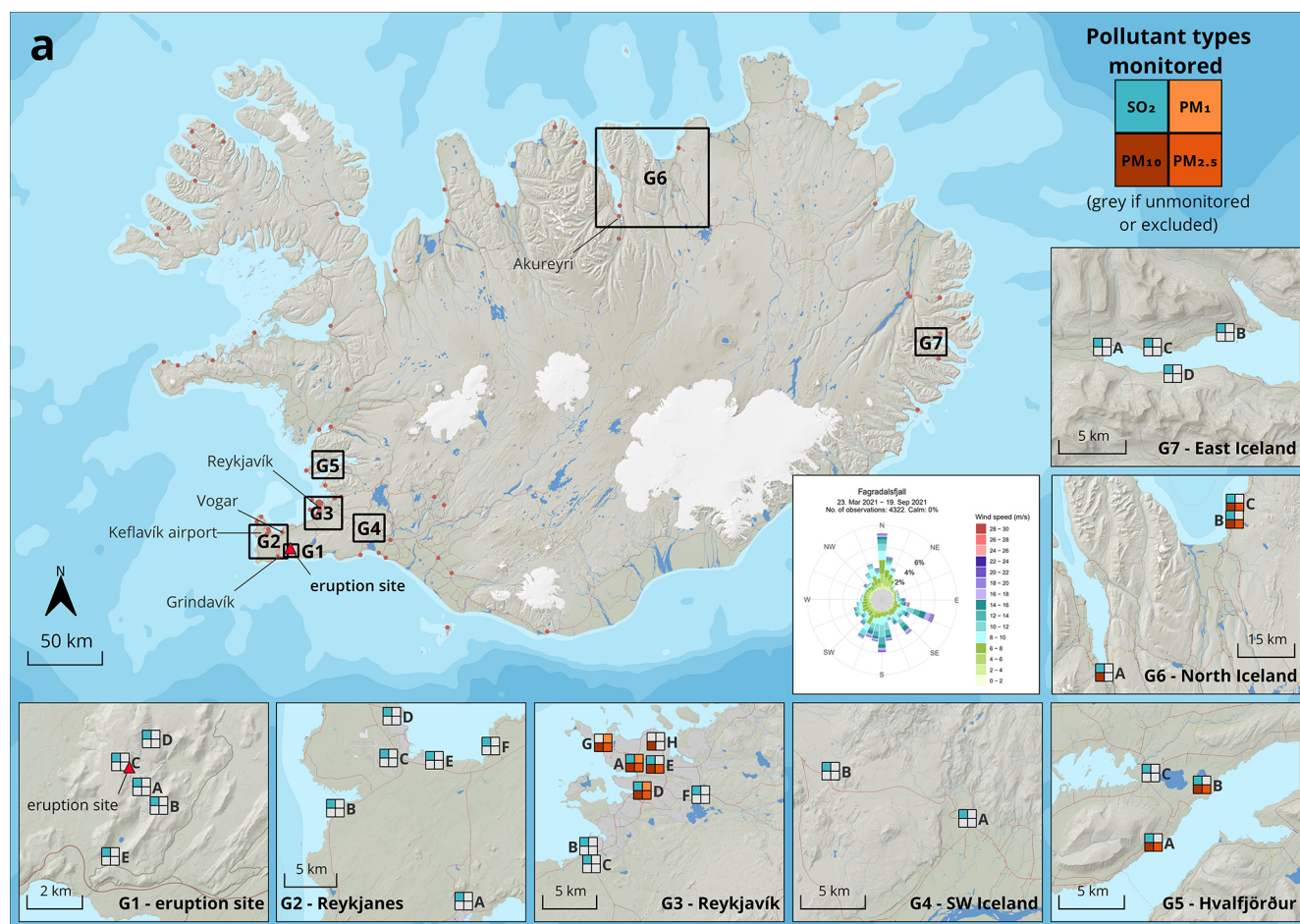
Figure 1. Map of Iceland showing the eruption site and air quality monitoring stations. Red circles on the main map show the location of populated areas, including the capital area Reykjavík which is represented with a comparatively larger circle. The stations were organised in seven geographic clusters (each shown on the enlarged insets). G1 – Eruption site (0–4 km from the eruption site). G2 – Reykjanes peninsula (9–20 km). G3 – Reykjavík capital area (25–35 km). G4 – Southwest Iceland (45–55 km). G5 – Hvalfjörður (50–55 km). G6 – North Iceland (A and B $\sim$ 280 km; C and D $\sim$ 330 km). G7 – East Iceland ($\sim$ 400 km). The map shows the air pollutant species monitored at each station (SO_2, PM_{10}, $PM_{2.5}$, PM_1). Areas G2–G7 were monitored with regulatory stations, while G1 was monitored using lower-cost eruption response sensors. Source and copyright of basemap and cartographic elements: Icelandic Met Office & Icelandic Institute of Natural History.

Since the 2021 eruption, eleven further eruptions have occurred on the Reykjanes peninsula: two within the Fagradalsfjall volcanic system (August 2022 and July 2023), and nine within the adjacent Reykjanes-Svartsengi system (December 2023 to August 2025). The 2021 eruption did not trigger significant wildfires; however, several subsequent episodes have caused extensive fires (primarily of vegetation but also some urban structures), warranting a dedicated investigation into their effects on air quality and related health outcomes. Volcanic unrest continues at the time of writing, and based on the eruption history of the Reykjanes peninsula, further eruptions may occur repeatedly over the coming decades or centuries.

2   Methods

Data were collected by two types of instrument networks:

1. A regulatory municipal air quality (AQ) network, managed by the Environmental Agency of Iceland (EAI), which measured SO_2 and particulate matter (PM) in different size fractions.

2. An eruption-response lower-cost sensor (LCS) network measuring SO_2 only, operated by the Icelandic Meteorological Office (IMO).

2.1   Regulatory municipal network

The regulatory network monitors air quality across Iceland in accordance with national legal mandates and complies with

Icelandic Directive (ID) regulations. Most of the monitoring stations are located in populated areas and measure a variety of air pollutants. Here, we analysed SO$_2$ and PM in the PM$_1$, PM$_{2.5}$, and PM$_{10}$ size fractions, which are the most important volcanic air pollutants with respect to human health in downwind populated areas (Stewart et al., 2021). Detection of SO$_2$ is based on pulsed ultraviolet fluorescence, and detection of PM is based on light scattering photometry and beta attenuation. The detection limits for the majority of the stations in this study were reported to be $\sim$ 1–3 µg m^{-3} SO$_2$ and < 5 µg m^{-3} PM$_{10}$. Station-specific instrument details, detection and resolution limits, and operational durations are in Table S1 in the Supplement. Figure 1 shows the location of the stations and the air pollutants species measured at each site.

2.2 Eruption site sensors

At the eruption site (0.6–3 km from the active craters), the Icelandic Meteorological Office (IMO) installed a network of five commercially available SO$_2$ LCS (Fig. A1) between April and July 2021 to monitor air quality. PM was not monitored with this network due to cost-benefit considerations. Two LCS sensor brands were used, Alphasense SO$_2$-B4 and Crowcon XGuard. The sensor specifications and operational durations are detailed in Table S1. Figure 1 shows the location of the eruption-response SO$_2$ sensor network. Stations A, B, and E were in close proximity to the public footpaths, while stations C and D were further afield to the north and northwest of the eruption site. The main purpose of the eruption-response network was to alert visitors when SO$_2$ levels were elevated and therefore potentially unhealthy. The measurements from the sensor network were publicly available in real-time on the EAI air quality monitoring website (https://airquality.is/, last access: 21 December 2025). The eruption site was staffed by members of the rescue services and/or rangers, who carried handheld SO$_2$ LCS to supplement the installed network. When any of the LCS reported SO$_2$ concentrations as elevated (potentially-above 350 µg m^{-3}) visitors were urged to relocate to areas with cleaner air. During the course of the 2021 eruption and subsequent events (2022–2025), SO$_2$ measurements from the LCS stations were also used by the IMO to produce hazard maps around the active and potential eruption sites, with hazard zones defined by the distances at which elevated SO$_2$ was detected (Icelandic Meteorological office, 2025).

The LCS were used to alert people to elevated SO$_2$ levels and were not used to report accurate SO$_2$ concentrations. This was because LCS are known to be significantly less accurate than regulatory instruments (Crilley et al., 2018; Whitty et al., 2022, 2020). Whitty et al. (2022) assessed the performance of SO$_2$ LCS specifically in volcanic environments (same or comparable sensor models to those used here) and found that they were frequently subject to interferences restricting their capability to monitor SO$_2$ in low con-

centrations. The sensor accuracy identified in the field study by Whitty et al. (2022) was significantly poorer than the detection limits reported by the manufacturer.

The sensors used in this study were not calibrated or co-located with higher-grade instruments during the field deployment as this network was set up ad hoc as part of an eruption crisis response by the IMO. The crisis was two-fold: the eruption itself, and the unprecedented crowding of people who wanted to view the eruption at very close quarters. Furthermore, the 2021 eruption occurred during national and international COVID-19 lockdowns, which reduced the capacity for field-based research and operations.

The absence of a regulatory-grade field calibration significantly limits the accuracy of LCS dataset, particularly at lower concentration levels. To partially mitigate this, two LCS units were co-located at station G1-B between 6 and 22 June 2021 to quantify inter-sensor uncertainty. The co-located sensors were of two types used in this study: Crowcon XGuard (deployed at G1-A throughout the monitoring period and at G1-B until 22 June) and Alphasense SO$_2$-B4 (deployed at G1-B from 22 June and at G1-C, D, and E for the entire period). The measured concentrations showed a strong linear correlation ($r^2 = 0.70$), but Alphasense reported lower values relative to Crowcon, with a correlation coefficient of 0.38 (Fig. A2). This coefficient was used to estimate the measurement uncertainty for the two sensor types, represented here as error bars on relevant figures. While the colocation experiment was useful for identifying uncertainty between sensor brands, it did not quantify variability among sensors of the same brand.

Given the calibration and co-location limitations, we do not report quantitative SO$_2$ concentrations from the LCS network. Instead, the data are presented as a qualitative indicator of whether concentrations were likely elevated – defined as exceeding 350 µg m^{-3} hourly mean – within the uncertainty of the sensors. This threshold is approximately two orders of magnitude above the manufacturer-reported detection limit, making it reasonable to assume that such levels were detectable. However, these values should be interpreted only as indicative; "elevated levels" do not represent confirmed air quality exceedances.

2.3 Data processing

SO$_2$ measurements were downloaded from 24 regulatory stations and 5 eruption site sensors, and PM$_{10}$, PM$_{2.5}$ and PM$_1$ were downloaded from 12, 11 and 3 regulatory stations, respectively. Data from the regulatory stations were quality-checked and, where needed, re-calibrated by the EAI. Where the operational duration was sufficiently long, we obtained SO$_2$ and PM measurements for both the eruption period and the non-eruptive background period.

We excluded from the analysis any regulatory stations that had data missing for more than 4 months of the eruption period (> 70 %). Further details on exclusion of individual

stations are in Table S1. These criteria excluded PM$_{10}$ and PM$_{2.5}$ from two stations (G3-B, G3-C); and PM$_{10}$ from one station (G3-H). Data points that were below instrument detection limits were set to 0 µg m^{-3} in our analysis. See Table S1 for the instrument detection limits of each instrument.

The eruption period was defined as 19 March 20:00 UTC/local time–19 September 2021 00:00 UTC/local time in agreement with Barsotti et al. (2023). The background period was defined differently for SO$_2$ and PM. For SO$_2$, the background period was defined as 19 March 2020 00:00 UTC/local time–19 March 2021 19:00 UTC/local time, i.e. one full calendar year before the eruption. Outside of volcanic eruption periods, SO$_2$ concentrations in Iceland are generally low with little variability due to the absence of other sources, as shown by previous work (Carlsen et al., 2021a; Ilyinskaya et al., 2017), and subsequently confirmed by this study. The only exception is in the vicinity of aluminium smelters where relatively small pollution episodes occur periodically. A one-year long period was therefore considered as representative of the background SO$_2$ fluctuations. We checked our background dataset against a previously published study in Iceland that used the same methods (Ilyinskaya et al., 2017) and found no statistically significant difference.

PM background concentrations in Iceland are much higher and more variable than those of SO$_2$. PM frequently reaches high levels in urban and rural areas, with significant seasonal variations (Carlsen and Thorsteinsson, 2021; Dagsson-Waldhauserova et al., 2014); the causes of this variability are discussed in the Results and Discussion. To account for this variability, we downloaded PM data for as many non-eruptive years as records existed, and analysed only the period 19 March 20:00 UTC/local time–19 September 00:00 UTC/local time in each year, i.e. the period corresponding to the calendar dates of the 2021 eruption. From here on, we refer to this period as "annual period". The annual periods in 2010, 2011, 2014, and 2015 were partially or entirely excluded from the non-eruptive background analysis due to eruptions in other Icelandic volcanic systems (Eyjafjallajökull 2010, Grímsvötn 2011, Holuhraun 2014–2015) and associated post-eruptive emissions and/or ash resuspension events. The annual period of 2022, i.e. the year following the 2021 eruption, was partially included in the background analysis: measurements between 19 March and 1 August 2022 were included, but measurements from 2 August 2022 onwards were excluded because another eruptive episode started in the Fagradalsfjall volcanic system. Since August 2022 there have been ten more eruptions in the same area at intervals of weeks-to-months, and therefore we have not included more recent non-eruptive background data. Although the 2022 annual period is only partially complete, it was particularly important for statistical analysis of PM$_1$ as operational measurements of this pollutant began only in 2020. The number of available background annual periods

for PM$_{10}$ and PM$_{2.5}$ varied depending on when each station was set up, ranging from 1 to 12 (Table S1).

The importance of non-volcanic sources of PM in Iceland meant that PM concentrations during the eruption period may have been elevated independently of volcanic activity. To identify the volcanic contribution to PM levels, we processed the data following a similar approach to Ilyinskaya et al. (2017). PM data were filtered to include only periods when SO$_2$ concentrations exceeded the non-eruptive background average; these periods are hereafter referred to as "plume-present days". Stations G3-G and G3-H did not monitor SO$_2$ and were filtered using SO$_2$ data from stations located within 2 km distance (G3-A and G3-E, respectively). This plume-identification approach has inherent strengths and limitations. First, it is effective at sites with negligible non-volcanic SO$_2$ sources, which applies to most of the monitored locations in Iceland; however, its reliability decreases near aluminium smelters, which represented a minor yet locally important SO$_2$ source at stations G5-all, G6-C, and G7-all. Second, it may exclude periods when the volcanic plume was present with low SO$_2$ but elevated PM, as can occur when the plume is chemically mature (Ilyinskaya et al., 2017). Third, it cannot distinguish between days when PM is predominantly sourced from an eruption and days when volcanic PM is strongly mixed with another PM source, such as dust storms. To address these uncertainties, we present both filtered and unfiltered PM datasets and compare them in our discussion.

Finally, we considered whether the year 2020 had lower PM$_{10}$ and PM$_{2.5}$ concentrations compared to other non-eruptive years due to COVID-19 societal restrictions and the extent to which this was likely to impact our results. The societal restrictions in Iceland were relatively light, for example, schools and nurseries remained open throughout. We found that the average 2020 PM$_{10}$ and PM$_{2.5}$ concentrations fell within the maximum-minimum range of the pre-pandemic years for all stations except at G3-E where PM$_{10}$ was 10 % lower than minimum pre-pandemic annual average, and PM$_{2.5}$ was 12 % lower; and at G5-A where PM$_{2.5}$ was 25 % lower (no difference in PM$_{10}$). G3-E is at a major traffic junction in central Reykjavík, and G5-A is on a major commuter route to the capital area. For PM$_1$, only one station was already operational before the COVID-19 pandemic (G3-A); PM$_1$ concentrations at this station were 20 % higher in 2020 compared to 2022 (post-pandemic). We concluded that PM data from 2020 should be included in our analysis but we note the potential impact of pandemic restrictions.

2.4 Data analysis

We organised the air quality stations into geographic clusters to assess air quality by region. The geographic clusters were the immediate vicinity of the eruption site (G1, 0–4 km from the eruption site), the Reykjanes peninsula (G2, 9–

20 km), the capital area of Reykjavík (G3, 25–35 km), South-west Iceland (G4, 45–55 km), Hvalfjörður (G5, 50–55 km), North Iceland (G6-A ~ 280 km; G6-B and C ~ 330 km), and East Iceland (G7, ~ 400 km), Fig. 1. Figures A3–A9 show SO$_2$ time series data for each individual station in geographic clusters G1–G7, respectively. Figures A10–A12 show PM time series data for each individual station in geographic clusters G3, G5 and G6, respectively.

For each station that had data for both the eruption and background periods, two-sample t-tests were applied to test whether the differences in background and eruption averages were statistically significant for the different pollutant species. For the eruption period, analyses were conducted separately for the full eruption duration and for plume-present days.

In addition to time series analysis, we analysed the frequency and number of events where pollutant concentrations exceeded air quality thresholds. Air quality thresholds are pollutant concentrations averaged over a set time period (usually 60 min or 24 h), which are considered to be acceptable in terms of what is robustly known about the effects of the pollutant on health. An air quality threshold exceedance is an event where the pollutant concentration is higher than that set out in the threshold. Evidence-based air quality thresholds have been defined for SO$_2$, PM$_{2.5}$ and PM$_{10}$, but not yet for PM$_1$, largely due to the paucity of regulatory-grade data on concentrations, dispersion and exposure (World Health Organization, 2021). For SO$_2$, most countries, including Iceland, use an hourly-mean threshold of 350 µg m^{-3}; and the threshold for the total number of exceedances in one year is 24 (Icelandic Directive, 2016). We used these thresholds for SO$_2$ in our study. The air quality thresholds for PM are based on 24 h averages, as there is currently insufficient evidence base for hourly-mean thresholds. For PM$_{10}$ we used the Icelandic Directive (ID) and World Health Organisation (WHO) daily-mean threshold of 50 µg m^{-3}, and for PM$_{2.5}$ we used the WHO daily-mean threshold of 15 µg m^{-3}, as no ID threshold is defined. While there are currently no evidence-based air quality thresholds available for PM$_1$, some countries, including Iceland use selected values to help communicate the air pollutant concentrations and their trends to the public. The Environment Agency of Iceland (EAI) uses a "yellow" threshold for PM$_1$ at 13 µg m^{-3} to visualise data from the regulatory stations and this value was used here (termed "EAI threshold").

To meaningfully compare the frequency of air quality threshold exceedance events for PM$_{10}$, PM$_{2.5}$ and PM$_1$ between the eruption and the non-eruptive background periods we normalised the number of exceedance events. This was done because the eruption covered only one annual period (see the definition of "annual period" in Sect. 2.3) but the number of available background annual periods varied between stations depending on how long they have been operational, ranging between 1 and 12 periods. We normalised by dividing the total number of exceedance events at a given

station by the number of annual periods at the same station. For example, for a station where the non-eruptive background was 6 annual periods the total number of exceedance events was divided by 6 to give a normalised annual number of exceedance events. The eruption covered one annual period and therefore did not require dividing. We refer to this as "normalised number of exceedance events" in the Results and Discussion. Table S1 contains summary statistics for all analysed pollutant means, maximum concentrations, number of air quality threshold exceedances, and number of background annual periods for PM data.

Three regulatory stations within geographic cluster G3 (Reykjavík capital area) measured all three PM size fractions (PM$_1$, PM$_{2.5}$ and PM$_{10}$), which allowed us to calculate the relative contribution of different size fractions to the total PM concentration. Since PM size fractions are cumulative, in that PM$_{10}$ contains all particles with diameters ≤ 10 µm, the size modes were subtracted from one another to determine the relative concentrations of particles in the following categories: particles ≤ 1 µm in diameter, 1–2.5 µm in diameter and 2.5–10 µm in diameter. The comparison of size fractions between the eruption and the background was limited by the relatively short PM$_1$ time series and our results should be re-examined in the future when more non-eruptive measurements have been obtained.

3 Results and discussion

3.1 Eruption-driven increase in PM$_1$ concentrations relative to PM$_{10}$ and PM$_{2.5}$

Emerging studies of the links between PM$_1$ and health impacts in urban air pollution have shown that even small increases in the PM$_1$ proportion within PM$_{10}$ can be associated with increasingly worse outcomes; e.g. liver cancer mortalities in China were found to increase for every 1 % increase in the proportion of PM$_1$ within PM$_{10}$ (Gan et al., 2025). Time series of PM$_1$, PM$_{2.5}$ and PM$_{10}$ concentrations were collected at three stations in the Reykjavík capital (G3-A, G3-D and G3-G, Fig. 1), allowing us to compare the relative contributions of the three size fractions in this area (25–35 km distance from the eruption site). All three stations exhibited low SO$_2$ concentrations during non-eruptive periods (both in mean values and variability), providing high confidence in detecting plume-present days (126 d at G3-A and G3-G, and 78 d at G3-D, out of 184 eruption days). When we considered the whole eruption period, all three stations showed a measurable increase in the average PM$_1$ mass proportion relative to PM$_{10}$ and PM$_{2.5}$ (Fig. 2). The proportion of PM$_1$ mass within PM$_{10}$ increased from the average of 16 %–24 % in the background (one standard deviation ± 7 %–13 %) to 24 %–32 % during the eruption (± 16 %–19 %); and within PM$_{2.5}$ from approximately 47% in the background to ~ 60 % during the eruption period. When considering only plume-present days (Fig. 2), the proportional increase in PM$_1$ was
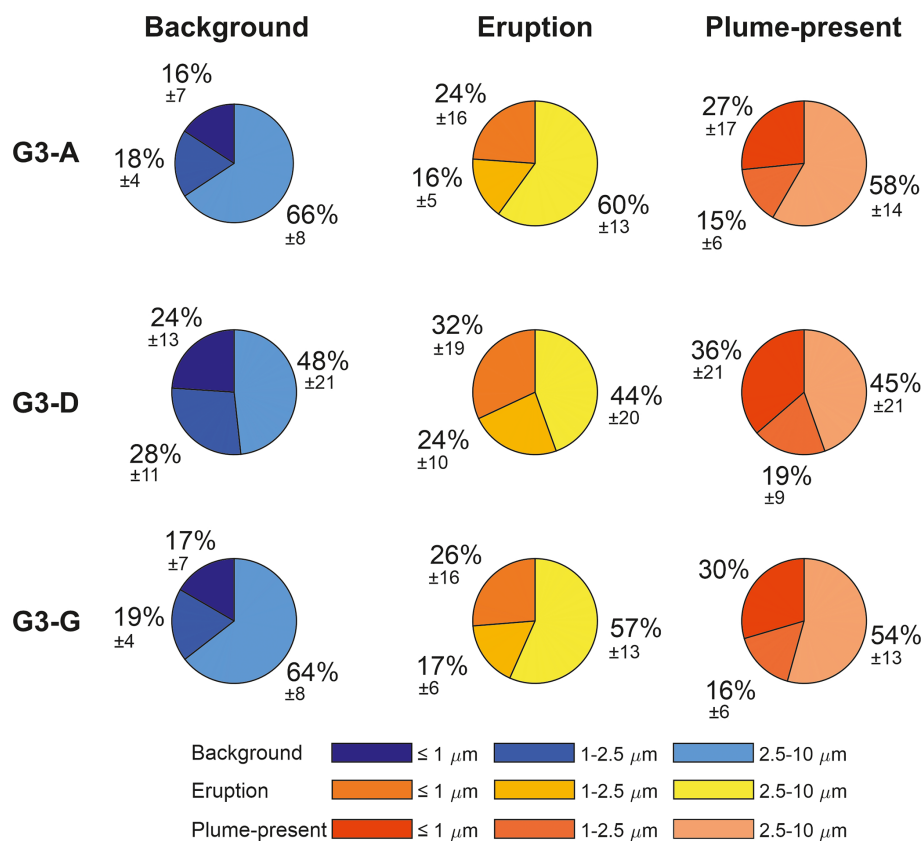
Figure 2. The relative contributions of three PM size fractions within PM_{10} (expressed as mass %) during the non-eruptive background, during the whole eruption period ("Eruption"), and on plume-present days only (see main text for the definition of "plume-present"). The size fractions shown are: PM $\leq 1\,\mu m$, PM $1–2.5\,\mu m$, and PM $2.5–10\,\mu m$ in diameter. The % mass is the mean $\pm 1\sigma$ standard deviation. G3-A, G3-D and G3-E were the stations in Iceland where all three size fractions were measured, all located within Reykjavík capital area.

even more pronounced – accounting for 27 %–36 % of PM_{10} – compared to background conditions, further highlighting the dominant influence of the volcanic source.

These are novel findings showing that volcanic plumes contribute a higher proportion of PM_1 relative to both PM_{10} and $PM_{2.5}$ when sampled at a distal location from the source (25–35 km in this study). When sampled at the active vent, volcanic plumes from basaltic fissure eruptions have been previously shown to contain a large amount of PM_1, but also a substantial proportion of coarse PM ($> 2.5\,\mu m$) (Ilyinskaya et al., 2017; Martin et al., 2011; Mason et al., 2021). At the vent, the composition of the fine and coarse size modes is typically very different: the finer fraction is primarily formed through the conversion of SO_2 gas into sulphate particles, whereas the coarser fraction consists of fragmented silicate material (i.e. ash), which may be present in small concentrations even in ash-poor fissure eruptions (Ilyinskaya et al., 2021; Mason et al., 2021). The conversion of SO_2 gas to sulphate particles continues for hours to days after emission, generating new fine particles over time (Green et al., 2019; Pattantyus et al., 2018). In contrast, ash particles are not replenished in the plume after emission and are progressively

removed through deposition. This may explain the elevated concentrations of particles in the finer size fractions observed downwind of the eruption site relative, to the coarser size fractions. These findings have implications for public health hazards, as volcanic plumes most commonly affect populated areas located tens to hundreds of kilometres from the eruption site.

3.2 Significant increases in average and peak pollutant levels

Most areas of Iceland, up to 400 km from the eruption site, recorded statistically significant increases in average and/or peak SO_2 and PM_1 concentrations during the eruption compared to the background period.

Figure 3 and Table 1 present SO_2 concentrations (hourly-means in $\mu g\,m^{-3}$), measured by regulatory stations across Iceland. During the non-eruptive background period, SO_2 concentrations at the majority of the monitored locations were low (long term average of hourly-means generally $< 2\,\mu g\,m^{-3}$), which is in agreement with previous studies (Ilyinskaya et al., 2017). Stations near aluminium smelters
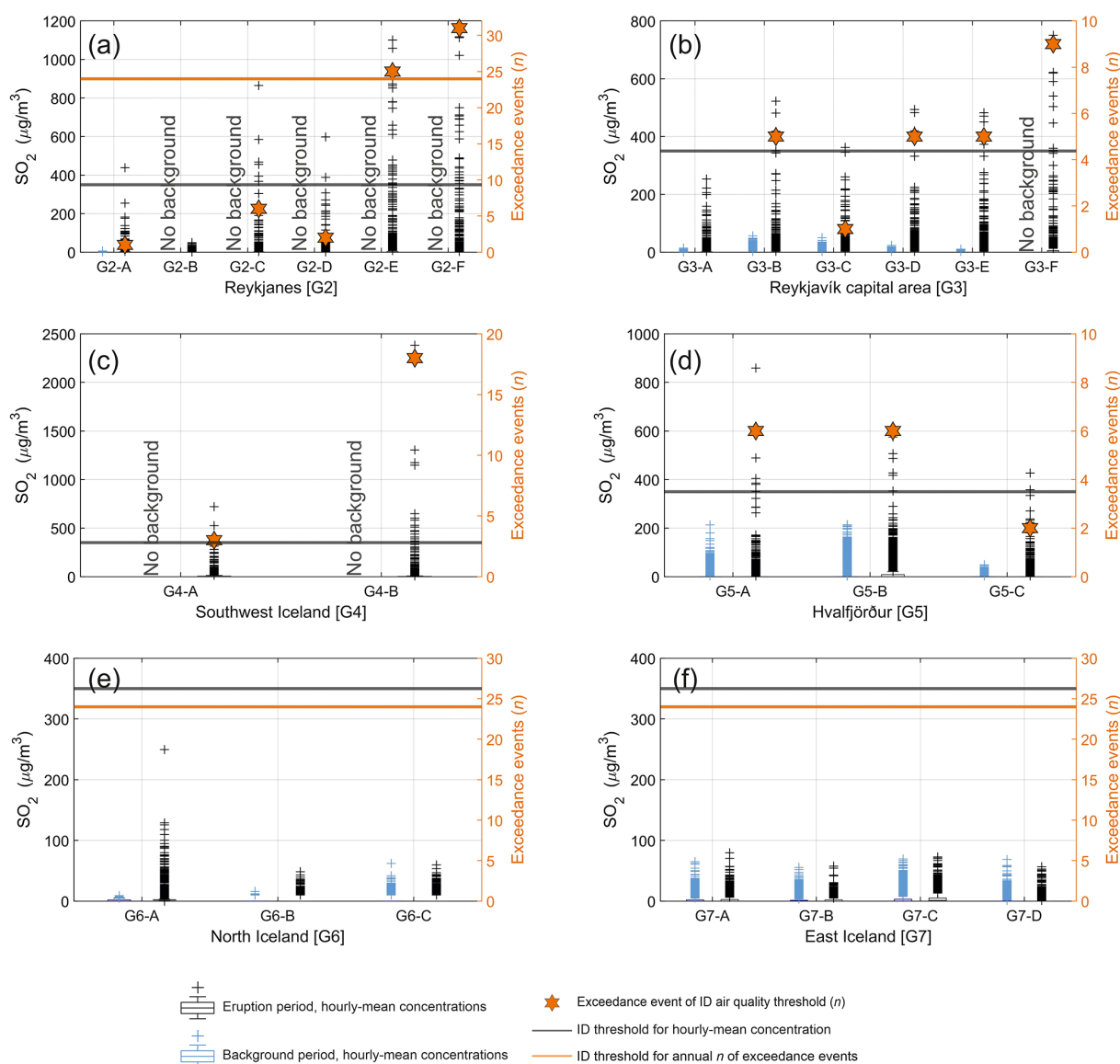
Figure 3. SO$_2$ hourly-mean concentrations (μg m^{-3}) and number of Icelandic Directive (ID) threshold exceedance events, measured by 24 regulatory-grade stations in populated areas in Iceland shown as six geographic clusters G2–G7 **(a–f)**. Pre-eruptive background data are shown for stations that were operational before the eruption began. The data are presented as box-and-whisker plots: boxes represent the interquartile range (IQR), the whiskers extend to $\pm 2.7\sigma$ from the mean, and crosses represent very high values (statistical outliers beyond $\pm 2.7\sigma$ from the mean). Note that the IQR is very low in most cases due to the negligible SO$_2$ concentrations in the local background; as a result, most of the SO$_2$ pollution episodes are statistical outliers. The ID air quality threshold of 350 μg m^{-3} hourly-mean is indicated by a black horizontal line in all panels. Orange stars represent the number of times this threshold was exceeded at each station ("Exceedance events"). The annual limit for cumulative hourly exceedance events is 24, shown by an orange horizontal line. Stations with orange stars above the orange line exceeded the annual threshold. Time series plots for each station are available in Appendix A.

(G5-all, G6-C, and G7-all) had higher long-term average values and periodically recorded short-lived escalations in SO$_2$ hourly-mean concentrations of several tens to hundreds μg m^{-3} during the background period (Fig. 3, Tables 1 and S1). The average SO$_2$ concentrations were higher during the eruption at all of the regulatory stations that had data from both before and during the eruption ($n = 16$), and the in-

crease was statistically significant ($p < 0.05$) at 15 out of the 16 stations (with the exception of G7-D near a smelter). The absolute increase in average SO$_2$ concentrations between the background and eruption period was relatively low, on the order of a few μg m^{-3} (Fig. 3 and Table 1). For example, the average concentration across the Reykjavík capital increased

from $0.32\,\mu g\,m^{-3}$ in the background to $4.1\,\mu g\,m^{-3}$ during the eruption.

The eruption period was also associated with substantial increases in peak SO_2 concentrations and number of air quality exceedance events across the populated areas. Figure 3 and Table 1 compare the background and eruption periods in terms of peak SO_2 concentrations and the number of exceedance events relative to the Icelandic Directive (ID) air quality threshold of $350\,\mu g\,m^{-3}$ hourly-mean. During the non-eruptive background period, SO_2 concentrations remained below the ID threshold at all 16 stations that were in operation. In contrast, during the eruption, 15 of the 24 stations recorded exceedances, with individual stations reporting between 0 and 31 events, generally highest near the eruption site. Two communities on the Reykjanes peninsula (G2) also exceeded the threshold for total exceedances in a one-year period (Fig. 3).

We attribute the combination of a relatively low absolute increase in average SO_2 concentrations and a large increase in peak concentrations to a combination of the dynamic nature of the eruption emissions (Barsotti et al., 2023; Pfeffer et al., 2024) and highly variable local meteorological conditions (wind rose for the eruption site in Fig. A13). These factors likely resulted in the volcanic plume being intermittently advected into populated areas, rather than acting as a continuous source of pollution.

Figures 4–6 and Table 2 show daily mean PM_{10}, $PM_{2.5}$ and PM_1 concentrations measured in the three regions with regulatory-grade monitoring (G3, G5, G6). Using above-background SO_2 as a proxy for plume presence, we identified 126 likely plume-affected days in the Reykjavík capital area (G3), 145 in Hvalfjörður (G5), and 40 in North Iceland (G6). Confidence is high for G3 due to the absence of local SO_2 sources, but lower for G5 and G6 because of nearby aluminium smelters; thus, plume-day counts for these areas should be considered maxima.

Some of the highest PM_{10} and $PM_{2.5}$ peaks in Reykjavík capital area (G3) during the eruption occurred on non-plume days (Fig. 4), notably in the periods 24–29 May and 3–4 June 2021. These two events accounted for most threshold exceedances – for example, five of seven for PM_{10} and four of six for $PM_{2.5}$ at station G3-A – and were recorded across all G3 stations, suggesting a diffuse distal source. The dominant non-volcanic PM source in Iceland is natural dust from highland deserts, with dust storms occurring frequently throughout the year with significant regional and seasonal variability (Butwin et al., 2019; Dagsson-Waldhauserova et al., 2014; Nakashima and Dagsson-Waldhauserová, 2019). We used back-trajectory analysis (HYSPLIT) and crowd-sourced observations to confirm that the PM_{10} and $PM_{2.5}$ peaks in Reykjavík on 24–29 May and 3–4 June were consistent with dust storms (Fig. A14).

When focusing on plume-present days, the frequency of PM_{10} and $PM_{2.5}$ exceedances in Reykjavík capital was comparable to or lower than background levels, indicating that ash-poor fissure eruptions are significant PM sources but not exceptionally high compared to other sources. In contrast, PM_1 peaks were strongly associated with plume days (Fig. 4), particularly during the time periods 2–6 July and 18–19 July 2021 (Figs. 7 and 8). We have high confidence in a volcanic origin of these events, supported by concurrent SO_2 peaks (up to $250\,\mu g\,m^{-3}$ hourly mean) and strong SO_2–PM_1 correlation (Figs. 7 and 8). PM_1 exceedances never exceeded the EAI threshold ($13\,\mu g\,m^{-1}$) during background periods, but during the eruption, exceedances occurred at all PM_1-monitoring stations, with up to four exceedances at G3-D on 19 July (Fig. 4; Table 2).

Presence of the volcanic plume was associated with a small but statistically significant increase in average PM_{10}, $PM_{2.5}$ and PM_1 concentrations in multiple locations. Average PM_1 concentrations were significantly higher at all monitored stations on plume-present days and throughout the eruption. $PM_{2.5}$ and PM_{10} averages were significantly higher at approximately half of the Reykjavík stations (G3) during plume-present days (Fig. 4). At these stations, PM_{10} increased from $\sim 9\,\mu g\,m^{-3}$ (background) to 12–$14\,\mu g\,m^{-3}$ during the eruption; $PM_{2.5}$ rose from ~ 3 to $\sim 5\,\mu g\,m^{-3}$; and PM_1 from 1.3–1.5 to $\sim 3\,\mu g\,m^{-3}$. Stations with significant increases in mean PM_{10} and $PM_{2.5}$ had cleaner backgrounds (peak daily means $< 90\,\mu g\,m^{-3}$ for PM_{10} and $< 20\,\mu g\,m^{-3}$ for $PM_{2.5}$), whereas stations without significant increases had peak daily means $\geq 160\,\mu g\,m^{-3}$ PM_{10} and $\geq 40\,\mu g\,m^{-3}$ $PM_{2.5}$. The higher-background stations were generally near roads with heavy traffic, suggesting that local sources – particularly traffic – were more influential for mean PM_{10} and $PM_{2.5}$ levels than the distal eruption.

Further afield, in Hvalfjörður (G5) and North Iceland (G6), all stations showed significantly higher $PM_{2.5}$ and PM_{10} concentrations on plume-present days compared to background (Figs. 5 and 6), though plume-day identification in these areas had lower confidence compared for G3 due to a higher SO_2 background.

The unequivocal eruption-related increase in both average and peak PM_1 concentrations indicates that volcanic fissure eruptions are among the most important – if not the dominant – sources of PM_1 in Iceland. Figure 9 and Table A1 compare PM_1 / PM_{10} ratios in Reykjavík under three scenarios: (1) volcanic plume presence, (2) two major Icelandic dust storms causing the highest PM pollution in 2021 (24–29 May and 3–4 June), and (3) representative eruption-free background periods. This comparison suggests distinct "fingerprint" ratios for the different PM sources: volcanic plume periods show the highest PM_1 / PM_{10} ratios (mean range 0.3–0.9), dust storms the lowest (mean range during storm peaks 0.04–0.05, mean range during the whole storm 0.1–0.3), and background conditions intermediate (mean ~ 0.2). These ratios may aid source attribution for PM episodes in Reykjavík and potentially other populated areas, especially when meteorological or visual observations are inconclusive. One limitation of this analysis is that PM_1

Table 1. SO$_2$ concentrations (hourly-mean, $\mu g\,m^{-3}$) in populated areas around Iceland during both the non-eruptive background and the Fagradalsfjall 2021 eruption. "Average" is the long-term mean of all stations within a geographic area $\pm 1\sigma$ standard deviation. "Peak" is the maximum hourly-mean recorded by an individual station within the geographic area. "ID exceedances" denotes the maximum number of times SO$_2$ concentrations (at any single station within a geographic area) exceeded the Icelandic Directive (ID) air quality threshold of $350\,\mu g\,m^{-3}$.

Geographic area	N of stations	Distance from eruption site (km)	SO$_2$ hourly-mean ($\mu g\,m^{-3}$)				ID exceedances (max n)	
			Background average $\pm$ standard deviation (1σ)	Eruption average $\pm$ standard deviation (1σ)	Background peak	Eruption peak	Background	Eruption
Reykjanes peninsula (G2)	6	9–20	0.13 ± 0.45	4.8 ± 44	7.7	2400	0	31
Reykjavík capital (G3)	6	25–35	0.32 ± 1.8	4.1 ± 21	57	750	0	9
South Iceland (G4)	2	45–55	No data	6.1 ± 44	No data	2400	No data	18
Hvalfjörður (G5)	3	50–55	3.9 ± 16	8.2 ± 28	210	860	0	6
North Iceland (G6)	3	280–330	0.41 ± 1.6	1.7 ± 6.3	9.1 at 280 km; 62 at 330 km	250 at 280 km; 48 at 330 km	0	0
East Iceland (G7)	4	400	1.7 ± 4.1	2.1 ± 4.9	69	79	0	0

measurements were only available in Reykjavík; whether volcanic PM$_1$ dominates in more distal communities remains to be investigated when high-quality datasets become available. Furthermore, data from winter eruptions are needed to assess seasonal variability in PM$_1$ sources. This analysis focused only on summer conditions due to the timing of the 2021 eruption. In urban areas, non-volcanic PM peaks are typically higher in winter, driven by tarmac erosion from studded tires (Carlsen and Thorsteinsson, 2021) and there are extreme spikes during New Year's fireworks and bonfires. Finally, we note that our study period included only two dust storms which cased elevated PM concentrations in Reykjavík. Different PM$_1$ / PM$_{10}$ ratios ($\sim$ 0.4–0.5) were reported for two dust storms affecting Reykjavík in 2015 (Dagsson-Waldhauserova et al., 2016), suggesting variability among these events and the need for further research.

The statistically significant increase in average PM$_{2.5}$ and PM$_{10}$ levels observed at least up to 300 km from the eruption site is remarkable, given the eruption's relatively small size and the prominence of non-volcanic PM sources in Iceland.

Historically, larger Icelandic fissure eruptions ($>$ 1 km^3 of erupted magma) have caused volcanic air pollution episodes far beyond Iceland – across mainland Europe during the 2014–2015 Holuhraun eruption (Schmidt et al., 2015; Twigg et al., 2016) and potentially even farther during the 1783–1784 Laki eruption (Grattan, 1998; Trigo et al., 2009). Simulations indicate that associated health impacts in Europe could have been substantial (Heaviside et al., 2021; Schmidt et al., 2011; Sonnek et al., 2017). During the recent Reykjanes eruptions (2021–2025), elevated volcanic SO$_2$ was detected at ground level by UK regulatory-grade stations on at least one occasion, in May 2024, exceeding previously docu-

mented levels at this distance (UKCEH, 2024). This suggests that PM concentrations may also have been elevated beyond Iceland during these events. Assessing the impacts of recent eruptions on air quality and public health in European and potentially more distant communities is therefore an important priority for future research.

3.3 Fine-scale temporal and spatial variability in SO$_2$ and PM$_1$ peaks

The dense regulatory monitoring network located 9–35 km from the eruption site (clusters G2 and G3, Fig. 1) revealed fine-scale variability in SO$_2$ concentrations at these relatively distal locations. Five out of six stations on the Reykjanes peninsula (monitoring SO$_2$ only) were positioned north and northwest of the eruption site, within the most common wind direction (wind rose in Fig. A13). Despite being only 3–16 km apart, two of these stations – G2-E and G2-F – recorded 25 and 31 hourly SO$_2$ exceedance events, respectively, while G2-B, G2-C, and G2-D recorded between 0 and 6 events (Fig. 3). To ensure this pattern was not an artifact of staggered station deployment, we recalculated exceedance events starting from 7 May 2021, the date by which all G2 stations were operational. The results remained consistent: G2-E and G2-F recorded 7 and 26 events, respectively, while G2-B, G2-C, and G2-D recorded between 0 and 6 events. The spatio-temporal difference between the two "high-exceedance" stations- – G2-E and G2-F, located within 5 km of each other – is also noteworthy. During the first seven weeks of the eruption (19 March–7 May 2021), G2-E recorded 18 of its 25 total exceedance events, while G2-F recorded only 5 of its 31.
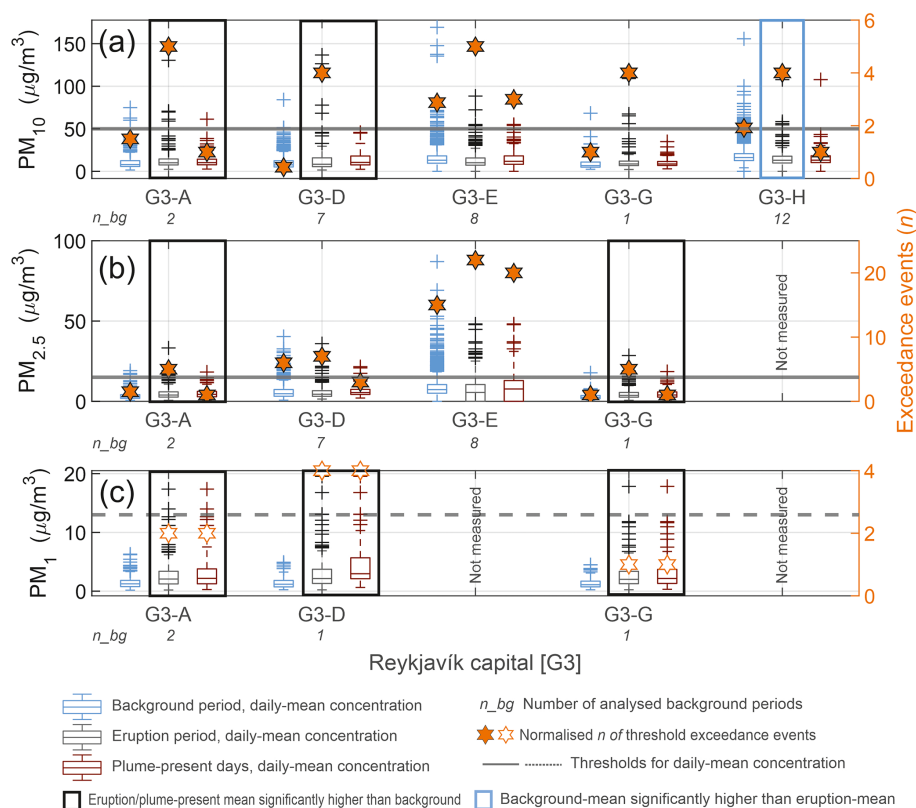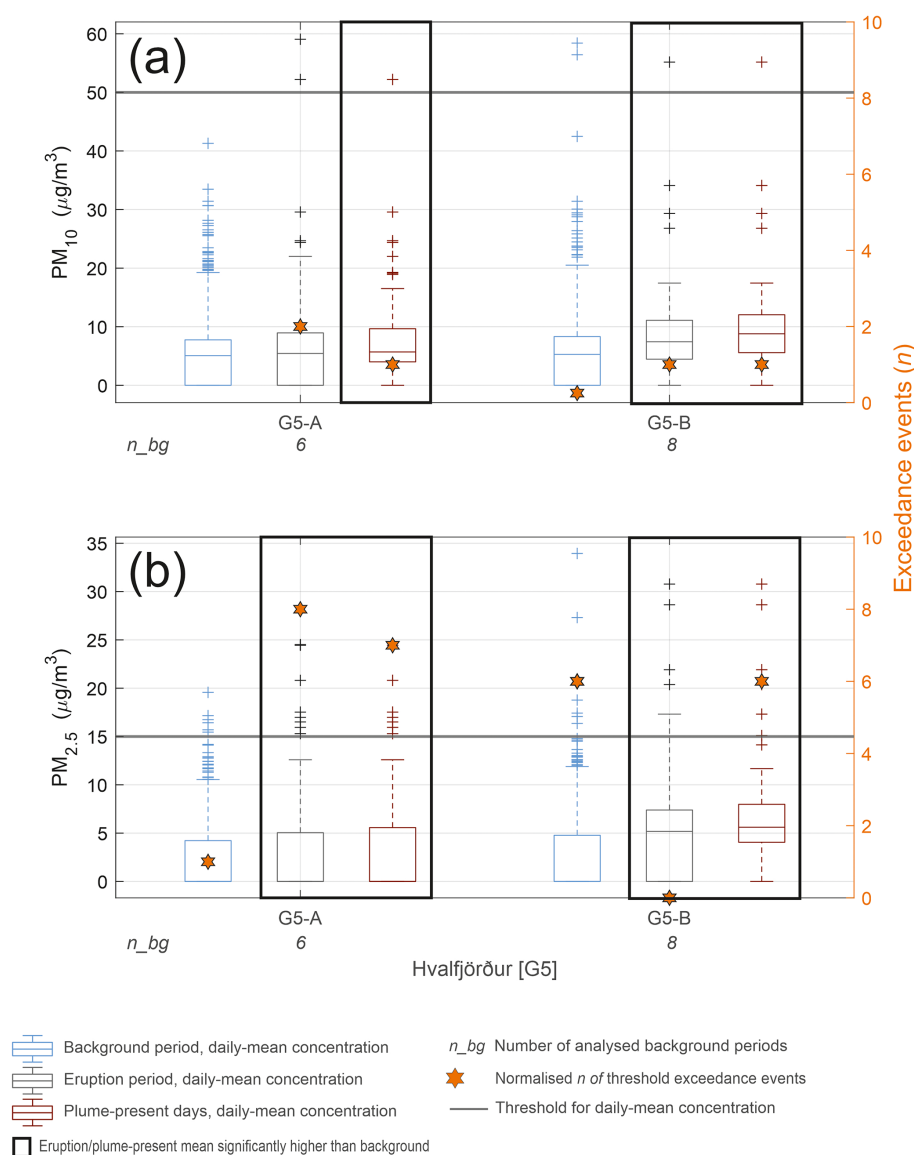
Figure 4. Daily-mean concentrations of **(a)** PM$_{10}$, **(b)** PM$_{2.5}$, and **(c)** PM$_1$ (µg m^{-3}) measured in the Reykjavík capital area during the non-eruptive background, during the whole eruption period, and on plume-present days only (see Methods for the definition of plume-present days). The data are presented as box-and-whisker plots, where boxes represent the interquartile range (IQR), the whiskers extend to $\pm 2.7\sigma$ from the mean, and crosses represent very high values (statistical outliers beyond $\pm 2.7\sigma$ from the mean). The median is shown with a horizontal line within each box. The value n_bg shown on the x axis indicates the number of background annual periods available for each station (see Methods for the definition of a background annual period). Stations where the average concentration during the eruption period and/or on the plume-present days was significantly higher ($p < 0.05$) than during the background are highlighted with a black box. The one station where the average concentration during the eruption period was significantly lower than during the background is highlighted with a blue box (G3-H). The absence of a box indicates no significant difference. Black solid line shows the Icelandic Directive (ID) air quality thresholds for PM$_{10}$ = 50 µg m^{-3} and PM$_{2.5}$ = 15 µg m^{-3} (24 h mean). Dashed black line shows the Environmental Agency of Iceland (EAI) threshold for PM$_1$ = 13 µg m^{-3} (24 h mean), a locally used threshold that is not internationally standardized. Stars with solid orange fill represent the normalised number of times PM$_{10}$ and PM$_{2.5}$ concentrations at each station exceeded the ID thresholds. Non-filled stars indicate the number of times PM$_1$ concentrations exceeded the EAI threshold. The number of the exceedance events is normalized to the length of the measurement period – refer to the main text for details on the normalization method. Time series plots for each station are available in Appendix A.

Figure 10 illustrates one such episode of fine-scale variability in SO$_2$ concentrations between the G2 stations on Reykjanes peninsula (28–30 May 2021). During this event, the volcanic pollution cloud "migrated" between the closely spaced stations G2-C, G2-D, and G2-E (separated by $\sim$ 2 km). The plume first reached G2-C, then shifted to G2-D and G2-E, with G2-D recording nearly twice the peak concentration of G2-E. This demonstrates that the edges of the volcanic pollution cloud at ground level were sharply defined.

Stations in the Reykjavík capital (area G3), located 25–35 km from the eruption site and within < 1–10 km of one another, also recorded fine-scale variability in pollutant con-

centrations – even at this relatively large distance from the source. The most significant volcanic plume advection episode in this area occurred on 18–19 July 2021, during which the G3 stations cumulatively recorded 21 SO$_2$ hourly mean air quality exceedance events – out of the 23 total exceedances recorded throughout the entire eruption. This episode revealed pronounced spatio-temporal variability in volcanic pollutant concentrations. Figure 7 illustrates the variation in SO$_2$ and PM$_1$ abundances during this episode, shown as time series (Fig. 7a and b) and as concentration ratios (Fig. 7c and d). This discussion focuses on PM$_1$ rather than PM$_{2.5}$ and PM$_{10}$ because PM$_1$ was more pronounced in the volcanic air pollution, as discussed in the previous sec-
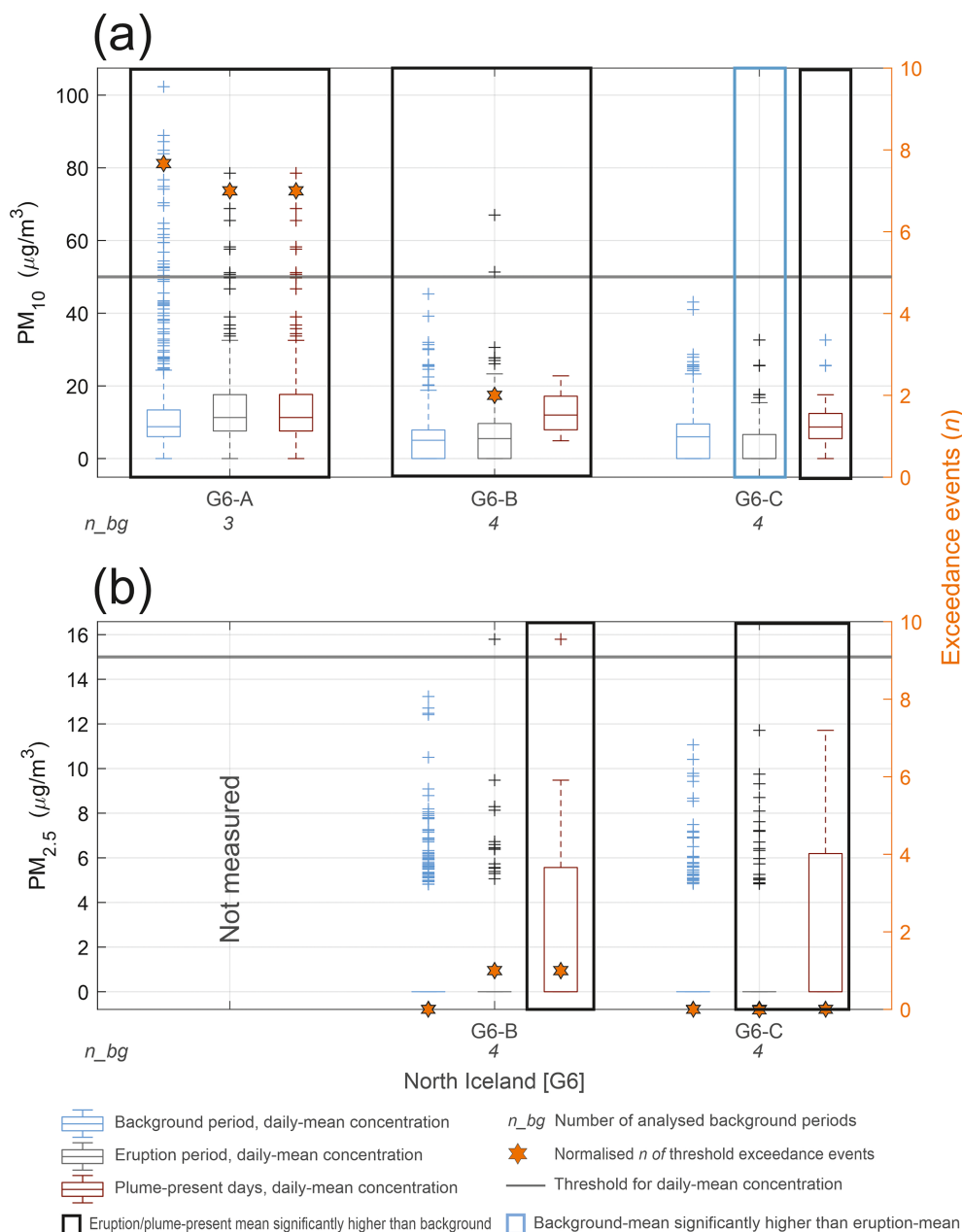
Figure 5. Daily-mean concentrations of **(a)** PM_{10}, and **(b)** $PM_{2.5}$ ($\mu g\,m^{-3}$), measured in the Hvalfjörður area during the non-eruptive background, during the whole eruption period, and on plume-present days only (see Methods for the identification of plume-present days). The data are presented as box-and-whisker plots, where boxes represent the interquartile range (IQR), the whiskers extend to $\pm 2.7\sigma$ from the mean, and crosses represent very high values (statistical outliers beyond $\pm 2.7\sigma$ from the mean). The median is shown as a horizontal line within each box; if the median line is absent, the value is zero. The value n_bg shown on the x axis indicates the number of background annual periods available for each station (see Methods for the definition of a background annual period). Stations where the average concentration during the eruption period and/or the plume-present days was significantly higher ($p < 0.05$) than during the background are highlighted with a black box. The absence of a box indicates no significant difference. Black solid line shows the Icelandic Directive (ID) air quality thresholds for $PM_{10} = 50\,\mu g\,m^{-3}$ and $PM_{2.5} = 15\,\mu g\,m^{-3}$ (24 h mean). Stars represent the normalised number of times PM_{10} and $PM_{2.5}$ concentrations at each station exceeded the ID thresholds. The number of the exceedance events is normalized to the length of the measurement period – refer to the main text for details on the normalization method. Time series plots for each station are available in Appendix A.

tions. Both SO₂ and PM_1 were significantly elevated above background levels at all G3 stations during the advection episode. Stations G3-A and G3-E, located within 1 km of each other, showed notable differences: G3-E recorded a maximum SO₂ concentration of $480\,\mu g\,m^{-3}$ and five exceedance events, while G3-A recorded a peak of $250\,\mu g\,m^{-3}$

and no exceedances (Figs. 3 and 7a). Similar fine-scale differences were observed in PM_1: for example, G3-D recorded up to twice the PM_1 hourly mean concentrations of G3-G during the same episode (Fig. 7b). The relative proportions of SO₂ and PM_1 during this episode also varied strongly between the two stations that measured both pollutants (G3-A

Figure 6. Daily-mean concentrations of **(a)** PM_{10}, and **(b)** $PM_{2.5}$ ($\mu g\,m^{-3}$), measured in North Iceland during the non-eruptive background, during the whole eruption period, and on plume-present days only (see Methods for the identification of plume-present days). The data are presented as box-and-whisker plots, where boxes represent the interquartile range (IQR); if a box is missing the 25th and 75th percentiles have the same value. The whiskers extend to $\pm 2.7\sigma$ from the mean, and crosses represent very high values (statistical outliers beyond $\pm 2.7\sigma$ from the mean). The median is shown as a horizontal line within each box; if the median line is absent, the value is zero. The value n_bg shown on the x axis indicates the number of background annual periods available for each station (see Methods for the definition of a background annual period). Stations where the average concentration during the eruption period and/or the plume-present days was significantly higher ($p < 0.05$) than during the background are highlighted with a black box. The one station where the average concentration during the whole eruption was significantly lower than during the background is highlighted with a blue box (G6-C). The absence of a box indicates no significant difference. Black solid line shows the Icelandic Directive (ID) air quality thresholds for $PM_{10} = 50\,\mu g\,m^{-3}$ and $PM_{2.5} = 15\,\mu g\,m^{-3}$ (24 h mean). Stars represent the normalised number of times PM_{10} and $PM_{2.5}$ concentrations at each station exceeded the ID thresholds. The number of the exceedance events is normalized to the length of the measurement period – refer to the main text for details on the normalization method. Time series plots for each station are available in Appendix A.
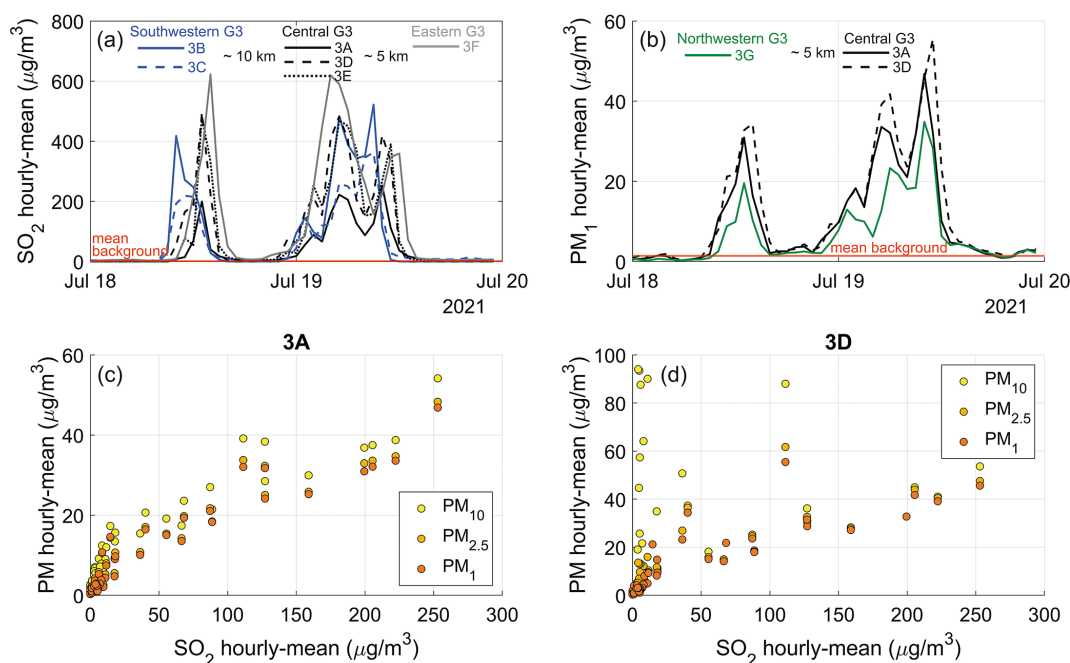
Figure 7. SO$_2$ and PM concentrations (µg m^{-3}, hourly-mean) during a "fresh" volcanic plume advection episode in the Reykjavík capital area (G3) on 18–19 July 2021. Stations G3-A to G3-F are regulatory monitoring sites, and the figure indicates their respective locations within Reykjavík (southwestern, central, eastern, and northwestern), along with approximate distances between them. **(a)** SO$_2$ hourly-mean time series. **(b)** PM$_1$ hourly-mean time series. **(c)** Scatter plot of concentrations of SO$_2$ and PM$_{10}$, PM$_{2.5}$ and PM$_1$ at station 3A, which measured all four pollutants. **(d)** Scatter plot of concentrations of SO$_2$ and PM$_{10}$, PM$_{2.5}$ and PM$_1$ at station 3D, which measured all four pollutants.

and G3-D). The peak hourly mean SO$_2$ concentration differed by nearly a factor of two between the stations (Fig. 7a), whereas peak PM$_1$ hourly means differed by no more than 20 % (Fig. 7b). During the advection episode, both pollutants exhibited three principal concentration peaks. The first peak, on 18 July at 13:00 UTC/local time, corresponded to the highest SO$_2$ concentration recorded at station G3-D. The final peak, on 19 July at 23:00 UTC/local time, marked the highest PM$_1$ concentration at the same station (Fig. 7a and b). Topographic elevation differences are unlikely to explain this spatial variability, as most G3 stations are located between 10 and 40 m a.s.l. (above sea level), with G3-F at 85 m a.s.l. One potential contributing factor could be the channelling or downwash of air currents by urban buildings – a process that may be particularly relevant in central Reykjavík. This warrants further investigation, such as through fine-scale dispersion modelling, but is beyond the scope of this study due to the challenges with accurately simulating relatively small volcanic plumes.

Figures S1 and S2 in the Supplement show animations of the simulated dispersion of volcanic SO$_2$ at ground level during the two pollution episodes discussed in this section, 28–30 May and 18–19 July 2021. The simulations were produced by a dispersion model used operationally for volcanic air quality advisories during the eruption by the Icelandic Meteorological Office (IMO) (Barsotti, 2020; Pfeffer et al.,

2024). As discussed by Pfeffer et al. (2024), the model had a reasonable skill in predicting the general plume direction but relatively low accuracy in simulating ground-level SO$_2$ concentrations for the 2021 eruption (Pfeffer et al., 2024).The model results are included here for qualitative purposes – as a binary yes/no indicator of potential plume presence at ground level. The sharp ground-level movement and boundaries of the plume during the 28–30 May episode were captured reasonably well by the model (Fig. S1), but the larger episode on 18–19 July was not reproduced by the model. This highlights the challenges of accurately simulating ground-level dispersion of volcanic emissions from eruptions like Fagradalsfjall 2021, as well as other small but highly dynamic natural and anthropogenic sources (Barsotti, 2020; Pfeffer et al., 2024; Sokhi et al., 2022). High-resolution observational datasets, including those presented here, can support improvements in dispersion model performance.

We also examined fluctuations in SO$_2$ and PM$_1$ during an advection episode of a chemically mature volcanic plume – locally known as *móða* (or *vog* in English, meaning volcanic smog) – in the Reykjavík capital area between 2 and 6 July 2021 (Fig. 8). A chemically mature plume has undergone significant gas-to-particle conversion of sulfur in the atmosphere and, as shown by Ilyinskaya et al. (2017), may be advected into populated areas several days after the initial emission. Compared to a fresh plume (Fig. 7c and d), the
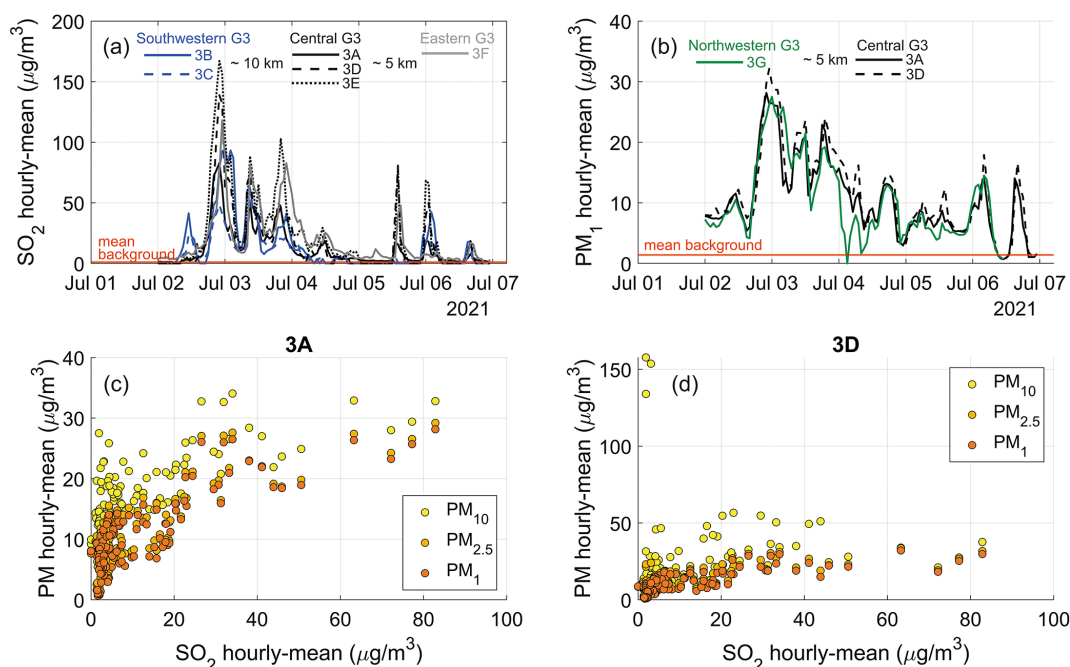
Figure 8. SO_2 and PM concentrations ($\mu g\,m^{-3}$) during a "mature" volcanic plume advection episode in Reykjavík capital area (G3) 2–6 July 2021. 3A to 3F are names of regulatory stations and the figure indicates their respective locations within Reykjavík (southwestern, central, eastern, and northwestern) and the approximate distance between them. **(a)** SO_2 hourly-means time series. **(b)** PM_1 hourly-means time series. **(c)** Scatter plot between concentrations of SO_2 and PM_{10}, $PM_{2.5}$ and PM_1 at station 3A, which measured all of these pollutants. **(d)** Scatter plot between concentrations of SO_2 and PM_{10}, $PM_{2.5}$ and PM_1 at station 3D, which measured all of these pollutants.

mature plume (Fig. 8c and d) is characterized by a higher PM/SO_2 ratio, with SO_2 elevated above background levels to a variable degree – sometimes only slightly (Ilyinskaya et al., 2017). Conditions that typically facilitate the formation and accumulation of *móða* include low wind speeds, high humidity, and intense solar radiation. Based on these factors, the 2–6 July episode was identified by the IMO as *móða* at the time of the event, and a public air quality advisory was issued. Figure 8c and d shows that during the *móða* episode, PM_1 was frequently elevated without a correspondingly high increase in SO_2. While SO_2 peaks were well-defined, PM_1 remained consistently elevated above background levels throughout the entire episode, with less prominent individual concentration peaks. This suggests that PM_1 may ground more persistently than SO_2 – an observation that could be tested in future studies using high-resolution dispersion modelling near the surface.

3.4 Estimates of population exposure and implications for health impacts

3.4.1 Exposure of residents

We assessed the frequency of exposure to SO_2 concentrations above the ID air quality threshold ($350\,\mu g\,m^{-3}$ hourly-mean) in populated areas G1, G2 and G3 using the data from the regulatory-grade network. Based on available evidence in

volcanic areas, exceedances of this threshold are associated with adverse health effects .(Carlsen et al., 2021a, b). The exceedance of the SO_2 air quality threshold was also a proxy for exposure to elevated PM concentration, since the volcanic pollution episodes contained elevated levels of SO_2, PM_1 and $PM_{2.5}$ – and to a lesser extent, PM_{10} (Figs. 7 and 8).
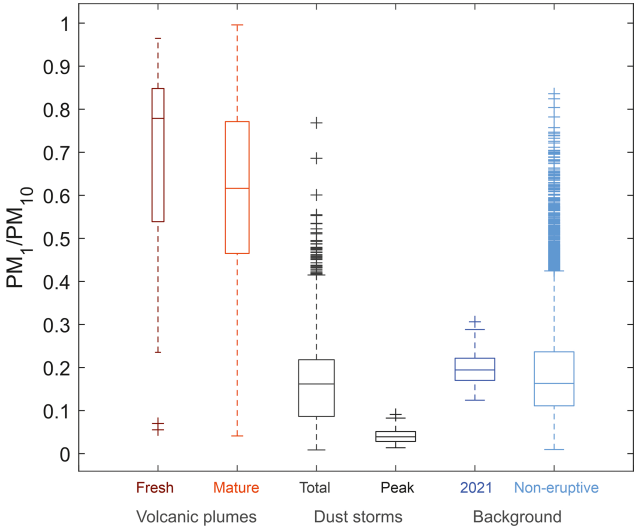
Population data for Iceland in the year 2020 were obtained from Statistics Iceland (2022) and were considered representative for 2021. Data were collected at the municipal level and included both total population and age-specific demographics. Municipality-level population datasets are relatively easy to obtain and are therefore frequently used in population exposure analyses (Caplin et al., 2019), but there are limitations to the resolution due to significant fine-scale spatial variations such as reported in this study.

In 2020, Iceland had a population of 369 000. Of this total, 6 % were aged ≤ 4 years and 15 % were aged ≥ 65 years – age groups which have been shown to be more vulnerable to volcanic air pollution (Carlsen et al., 2021a, b). A total of 263 000 people – equivalent to 71 % of the national population – resided within 50 km of the Fagradalsfjall eruption site, where most SO_2 air quality threshold exceedances occurred. Figure 11 presents municipality-level population data for this area, including total population and density, the number and density of individuals in vulnerable age groups, the locations

Table 2. PM_{10}, $PM_{2.5}$ and PM_1 concentrations ($\mu g\,m^{-3}$, 24 h mean) in populated areas around Iceland during both the non-eruptive background ("BG"), the whole eruption period ("Eruption"), and on "plume present" days only (see Methods for the definition of plume-present days). "Average" refers to the long-term mean of 24 h values of all stations within a geographic area $\pm 1\sigma$ standard deviation. "Peak" is the maximum 24 h-mean recorded by an individual station within the geographic area. "AQ exceedances" denotes the maximum number of times PM concentrations (at any single station within a geographic area) exceeded the following thresholds: PM_{10} – 50 $\mu g\,m^{-3}$; $PM_{2.5}$ – 15 $\mu g\,m^{-3}$; PM_1 – 13 $\mu g\,m^{-3}$.

Geographic area	n of stations (PM_{10}, $PM_{2.5}$, PM_1)	Distance from eruption site (km)	PM_{10} Average Bg	PM_{10} Average Eruption	PM_{10} Average Plume present	PM_{10} Peak Bg	PM_{10} Peak Eruption	PM_{10} Peak Plume present	PM_{10} AQ Bg	PM_{10} AQ Eruption	PM_{10} AQ Plume present	$PM_{2.5}$ Average Bg	$PM_{2.5}$ Average Eruption	$PM_{2.5}$ Average Plume present	$PM_{2.5}$ Peak Bg	$PM_{2.5}$ Peak Eruption	$PM_{2.5}$ Peak Plume present	$PM_{2.5}$ AQ Bg	$PM_{2.5}$ AQ Eruption	$PM_{2.5}$ AQ Plume present	PM_1 Average Bg	PM_1 Average Eruption	PM_1 Average Plume present	PM_1 Peak Bg	PM_1 Peak Eruption	PM_1 Peak Plume present	PM_1 AQ Bg	PM_1 AQ Eruption	PM_1 AQ Plume present
Reykjavík capital (G3)	5, 4, 3	25–35	15 ± 11	14 ± 14	14 ± 10	170	140	110	2.9	5	3	6.6 ± 6.8	5.7 ± 6.2	6.3 ± 6.3	87	48	48	15	22	20	1.4 ± 0.94	2.8 ± 2.6	3.4 ± 3.0	6.3	20	20	0	4	4
Hvalfjörður (G5)	3	50–55	5.6 ± 5.7	7.3 ± 7.8	8.3 ± 7.7	58	59	55	0.25	2	1	2.1 ± 3.4	3.9 ± 5.3	4.7 ± 5.5	34	31	31	1	8	7	No data								
North Iceland (G6)	3	280–330	7.7 ± 10	8.9 ± 11	14 ± 12	100	79	79	7.7	7	7	0.53 ± 1.9	0.71 ± 2.2	3.0 ± 4.0	13	16	16	0	1	1									

Figure 9. Variability in PM_1 / PM_{10} concentration ratios associated with different pollution sources in the Reykjavík capital area. Data represent hourly-means from stations measuring both size fractions (G3-A, G3-D, G3-G) and are shown as box-and-whisker plots: boxes indicate the interquartile range (IQR), whiskers extend to $\pm 2.7\sigma$ from the mean, and crosses mark statistical outliers beyond this range. The median is shown as a horizontal line within each box. "Volcanic plumes": periods during the 2021 eruption when the plume was advected toward Reykjavík (for definitions of "fresh" and "mature" plumes see Sect. 3.3). Data include one prolonged fresh plume event (> 24 h) and three discrete mature plume events, as mature plumes exhibit greater variability in PM size ratios (Ilyinskaya et al., 2017). "Dust storms": two Icelandic highland desert storms ($\sim 200\,km$ source distance) affecting Reykjavík in 2021; "total" refers to the full duration of dust storm events with PM above background ($PM_{10} > 10\,\mu g\,m^{?-3}$), while "peak" includes only hours with highly elevated PM ($PM_{10} > 50\,\mu g\,m^{?-3}$). "Background": representative summer conditions; "2021" refers to eruption-period without volcanic plume influence; "Non-eruptive" covers summer periods in 2020 and 2022. Table A1 provides the event timings and mean ratios for PM_1 / PM_{10}, $PM_1 / PM_{2.5}$ and $PM_{2.5} / PM_{10}$.

of hospitals, and the number of ID air quality threshold exceedances recorded at monitoring stations.

The Reykjavík capital area had approximately 210 000 residents (60 % of the total population), a high density of individuals in the potentially more vulnerable age groups, and a large number of hospitals (area G3 on Fig. 11). Air quality stations in this densely populated capital area recorded between 0 and 9 threshold exceedance events during the eruption period. Fine-scale spatial differences in ground-level pollutant concentrations (discussed in Sect. 3.3) may have played a critical role in determining people's exposure. For example, one of the largest hospitals in the country was located approximately equidistant ($\sim 2\,km$) from stations G3-A and G3-E, which recorded 0 and 5 SO_2 exceedance events, respectively. As a result, it remains unknown how frequently
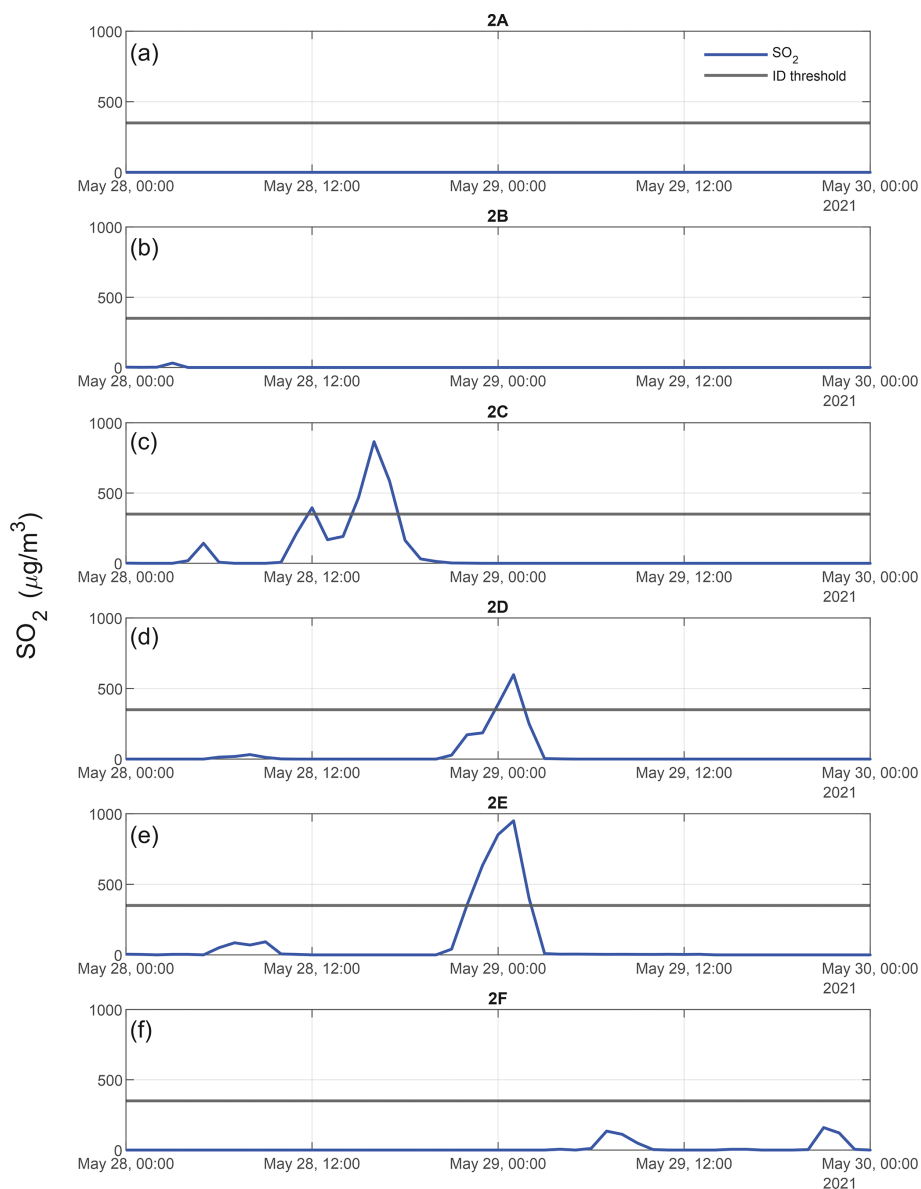
Figure 10. Spatial and temporal variability in SO$_2$ concentrations (μg m^{-3}, hourly-mean) between monitoring stations on the Reykjanes peninsula (G2) during 28–30 May 2021. The Icelandic Directive (ID) air quality threshold for hourly SO$_2$ concentrations ($350\,\mu$g m^{-3}) is indicated by a black horizontal line. **(a)** Station G2-A. **(b)** Station G2-B. **(c)** Station G2-C. **(d)** Station G2-D. **(e)** Station G2-E. **(f)** Station G2-F.

individuals at the hospital were exposed to above-threshold SO$_2$ levels. Similarly, the hospital closest to the eruption site – located about 20 km away – was situated between two monitoring stations, G2-D and G2-E, which recorded markedly different numbers of exceedance events: 2 and 25, respectively (Fig. 11). These examples highlight the importance of spatial resolution in air quality monitoring for accurately assessing population exposure.

The most frequent exposure to potentially unhealthy SO$_2$ levels occurred predominantly within a 20 km radius of the eruption site, particularly in municipalities on the Reykjanes

peninsula (Fig. 11). In this area (G2), up to 31 exceedance events were recorded – surpassing the annual threshold of 24 exceedances ($n = 24$). However, exposure estimates based solely on place of residence may not fully capture individual exposure, especially for working adults who commute. For example, station G2-A in the township of Grindavík recorded only one exceedance event, yet many residents worked at Keflavík Airport, where higher SO$_2$ levels were observed (five exceedance events at station G2-C). Conversely, residents in the town of Vogar (station G2-E, 25 exceedance events) who may have commuted to the Reyk-
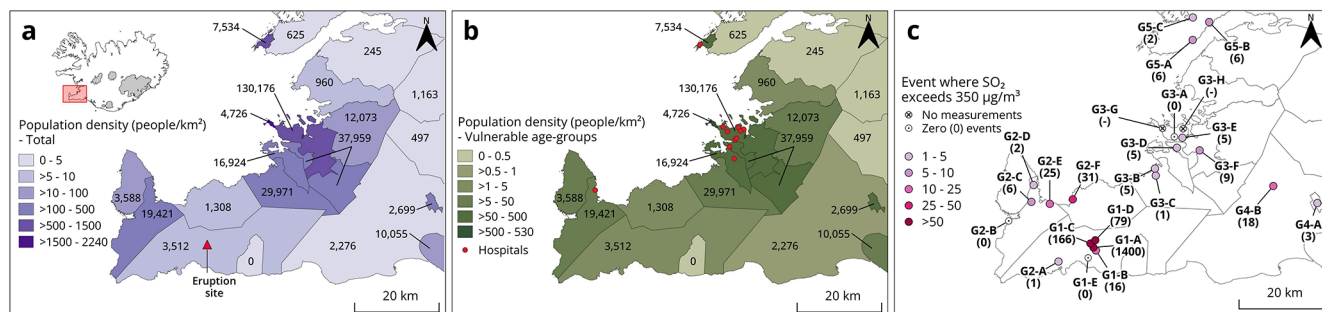
Figure 11. Potential exposure of the residents in the densely populated southwestern part of Iceland, including the Reykjavík capital area (G3) to above-threshold SO$_2$ concentrations. Population data are from Statistics Iceland for 2020. **(a)** The number of residents and the population density at the municipality level. The number of residents is shown for each municipality, and the colour scale represents the population density (n of people per km^2 in each municipality). **(b)** Potentially vulnerable age groups (≤ 4 years and ≥ 65 years of age). The number of people in the vulnerable age groups is shown for each municipality, and the colour scale represents the population density (n of people per km^2 in each municipality). The map also shows the location of hospitals. **(c)** Number of times when the SO$_2$ concentrations exceeded the ID air quality threshold of 350 µg m^{-3} hourly-mean during the eruption period as measured by the regulatory stations in areas G1, G2 and G3. Source and copyright of basemap and cartographic elements: Icelandic Met Office & Icelandic Institute of Natural History.

javík capital area – where fewer exceedances were recorded (0–9 events) – may have experienced lower actual exposure than estimated based on residence alone. In contrast, exposure estimates for children are likely more accurate, as most attend schools within walking distance or a short commute from home. The same applies to long-term hospital inpatients, whose exposure is closely tied to the location of the healthcare facility.

From a nationwide public health perspective, it was fortunate that volcanic pollutants were predominantly transported to the north and northwest of the eruption site. This atmospheric transport pattern likely mitigated the frequency of SO$_2$ pollution episodes in the densely populated capital area, situated to the northeast of the eruption site. Figure S3 illustrates the total probability of above-threshold SO$_2$ concentrations at ground level during the eruption, as simulated by the IMO dispersion model (Pfeffer et al., 2024). As outlined in Sect. 3.3, these simulations are used here solely to provide a qualitative indication of the broad plume direction at ground level. The modelled dispersion patterns are consistent with observational data, indicating that the plume most frequently grounded to the north and northwest of the eruption site, and more rarely in the capital area (Fig. S3).

Based on the available evidence, it is possible that the 2021 eruption may have led to adverse health impacts among exposed populations. Epidemiological studies by Carlsen et al. (2021a, b) on the 2014–2015 Holuhraun eruption demonstrated a measurable increase in healthcare utilisation for respiratory conditions in the Reykjavík capital area, associated with the presence of the volcanic plume. Exposure to above-threshold SO$_2$ concentrations was linked to approximately 20 % increase in asthma medication dispensations and primary care visits. During the Fagradalsfjall eruption, SO$_2$ concentrations in populated areas reached levels broadly comparable to those observed during the larger but more dis-

tal Holuhraun eruption. Holuhraun emissions led to 33 exceedances of the SO$_2$ air quality threshold in Reykjavík, with hourly-mean concentrations peaking at 1400 µg m^{-3} (Ilyinskaya et al., 2017). In comparison, the Fagradalsfjall eruption caused 31 exceedances, with a maximum of 2400 µg m^{-3} SO$_2$ recorded in the community of Vogar (station G2-F). Up to 18 SO$_2$ threshold exceedances were also recorded in areas within approximately 50 km of the eruption site (areas G1–G5). All areas that recorded above-threshold pollutant concentrations may have experienced adverse health effects.

Although the monitored regions in North and East Iceland (areas G6 and G7) did not register threshold exceedances, potential adverse health impacts in these areas cannot be ruled out. As reported by Carlsen et al. (2021b), even relatively small above-background increases in SO$_2$ levels during Holuhraun were associated with small but statistically significant rises in healthcare usage – approximately a 1 % increase per 10 µg m^{-3} SO$_2$ – suggesting the absence of a safe lower threshold.

Given the limited number and scope of health impact studies on previous volcanic eruptions, the potential health implications discussed here should be further investigated through dedicated epidemiological and/or clinical studies focused specifically on the Fagradalsfjall event. Moreover, existing health studies from volcanic regions have primarily concentrated on short-term exposure (hourly and daily), with a gap in research of potential long-term effects. Since the 2021 eruption, 11 additional eruptions of similar style and in the same geographic area have occurred. Although each event has been relatively short-lived – ranging from several days to several months – their cumulative impact on public health may be chronic as well as acute, and thus warrants comprehensive investigation.

Carlsen et al. (2021a) found that when volcanic air pollution events from the Holuhraun eruption were success-

fully forecast and public advisories were issued, the associated negative health impacts were reduced compared to events that were not forecast. In Iceland, residential buildings are predominantly well-insulated concrete structures with double-glazed windows, offering substantial protection from outdoor air pollution. However, under normal conditions, windows are kept open for ventilation, facilitated by the availability of inexpensive geothermal heating. Additionally, it is common practice for infants to nap outdoors in prams, and for school-aged children to spend breaks outside. Public advisories included simple, easily implemented measures such as keeping windows closed and minimizing outdoor exposure for vulnerable individuals. Given that such basic societal actions have been shown to be effective, it is likely that further improvements in pollution detection – particularly enhancements in spatial resolution – and more effective communication strategies could provide additional protection to the population.

3.4.2　Exposure of eruption site visitors

An interesting aspect of the eruption was that it was generally considered a very positive event by the Icelandic public (Ilyinskaya et al., 2024), and even though it took place in an uninhabited location the site became akin to a densely populated area due to the extremely high number of visitors. The mountainous area had no infrastructure before the eruption and was only accessible by rough mountain tracks. It was unsuitable for an installation of a regulatory air quality network but there were serious concerns about the hazard posed to the visitors by potentially very high SO$_2$ concentrations. In response, national and local authorities undertook significant efforts to mitigate hazards associated with both volcanic activity and general outdoor hazards. A network of three footpaths was established, originating from designated parking areas (Fig. 12). These footpaths were modified multiple times throughout the eruption as the lava field expanded and optimal viewing locations shifted (Barsotti et al., 2023). In this study, we evaluate the deployment of eruption-response LCS as a means to minimize exposure to hazardous SO$_2$ levels.

Automated footpath counters were installed by the Icelandic Tourist Board on 24 March 2021, with one device placed on each of the main footpaths leading to the eruption site and designated viewpoints (Fig. 12). These counters (PYRO-Box by Eco Counter) have a reported accuracy of 95 % and a sensing range of 4 m. The visitor numbers presented here represent a minimum estimate. While the majority of visitors used the established footpath network, some individuals may have walked outside the detection range of the counters and were therefore not recorded. Additionally, visitors arriving via helicopter sightseeing tours, children being carried, and individuals with authorized vehicle access (e.g., scientists and rescue personnel) were not included in the count. The visitor data also lacked demographic information, preventing any assessment of exposure among more vulnerable age groups. In addition, there is no data on whether people visited the eruption multiple times and were therefore potentially cumulatively more exposed. During the visitor-counting period (24 March to 18 September 2021), the eruption site was visited by approximately 300 000 people, averaging 1600 visitors per day (Fig. 12). The highest visitor numbers occurred in the early weeks of the eruption, coinciding with the Easter holiday period, with a daily average of 3300 visitors and a peak of 6000 on 28 March.

The five eruption-response LCS were strategically deployed along the main footpaths (Fig. 12a) to ensure proximity to visitors. Figure 12b shows the number of times at each LCS station that hourly-mean SO$_2$ was recorded as elevated (see Sect. 2.2 for definition of "elevated" and the sensor uncertainty). There was high variability between the stations, and therefore high variability in the potential exposure of the visitors to elevated SO$_2$ depending on where they were. Station G1-A, located closest to the active craters, recorded elevated SO$_2$ between 600 and 1600 times. Stations G1-B, G1-C, and G1-D recorded elevated SO$_2$ between 20 and 110 times, while G1-E did not register any highly elevated periods. Stations G1-C and G1-D were more frequently located downwind of the active vents, as supported by the wind rose diagram in Fig. A13. Additionally, based on visual observations during this eruption and similar fissure eruptions, a volcanic plume can occasionally collapse and spread laterally. This leads to extremely high concentrations of SO$_2$ even at locations in close vicinity of but upwind of the volcanic vent.

During the course of the 2021 eruption and subsequent events (2022–2025), SO$_2$ measurements from the LCS stations were used by the IMO to produce hazard maps around the active and potential eruption sites, with hazard zones defined by the distances at which elevated SO$_2$ was detected (Icelandic Meteorological office, 2025). Visitors were clearly advised to remain upwind of the active craters and lava field. The site was staffed by members of the rescue services and/or rangers, who carried handheld SO$_2$ LCS to supplement the semi-permanent sensor network. When SO$_2$ concentrations became elevated, and therefore potentially unhealthy, visitors were urged to relocate to areas with cleaner air. Although no formal health impact studies have been published to date, anecdotal reports in the Icelandic media suggest that only a small number of individuals sought medical attention after visiting the eruption site, citing symptoms related to gas exposure. This likely represents a very small proportion of the total visitor population. Instances of exposure to unhealthy SO$_2$ levels may have occurred for several reasons: not all visitors were in proximity to a sensor during their visit, and rapid shifts in wind direction or changes in eruption dynamics occasionally transported SO$_2$ into areas that had previously been unaffected.

In conclusion, the deployment of the LCS network at the eruption site for the purposes of alerting people to potentially-high SO$_2$ concentrations was likely valuable given the high frequency of elevated SO$_2$ concentrations and
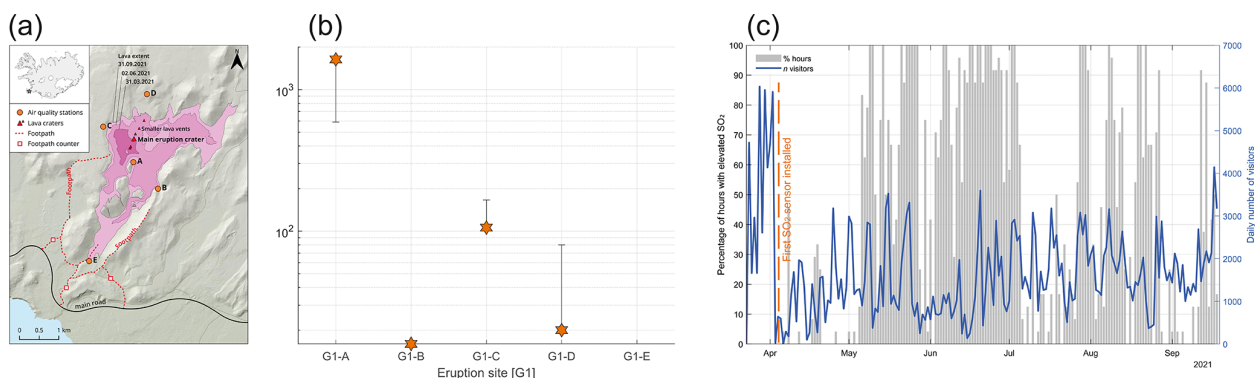
Figure 12. Visitor numbers and potential exposure to elevated SO$_2$ at the Fagradalsfjall eruption site between 24 March and 18 September 2021. **(a)** Topographic map of the eruption site showing crater locations, the evolving lava field extent, five LCS stations (A–E), primary visitor footpaths, and footpath visitor counters. **(b)** Total hours with elevated SO$_2$ concentrations recorded at each LCS station. Error bars indicate measurement uncertainty; the y axis is logarithmic. **(c)** Daily visitor counts (n of people) and daily percentage of time with elevated SO$_2$ (elevated hours/24×100). Grey bars show the daily max–min range across the five LCS stations. The LCS data should be interpreted only as indicative; "elevated SO$_2$" levels do not represent confirmed air quality exceedances. Source and copyright of basemap and cartographic elements: Icelandic Met Office & Icelandic Institute of Natural History.

the large number of visitors in a confined area. However, the absence of regulatory-grade calibration prevented any quantitative assessment of individual exposure to hazardous pollutants. To obtain high-quality datasets with LCS, regular and frequent field calibration against regulatory instruments is essential. However, such calibration is typically feasible only during short-term campaigns at reasonably accessible locations. In this crisis-response scenario, the challenging terrain and limited accessibility of the eruption site precluded field calibration. The primary concerns associated with uncalibrated LCS in emergency contexts are false negatives – where the sensor underreports concentrations that exceed health thresholds – and false positives – where the sensor overreports concentrations that are actually below threshold. False negatives pose a problem by failing to alert individuals to hazardous conditions, while repeated false positives may undermine public trust and reduce compliance with safety advisories.

4 Conclusions

The 2021 eruption of Fagradalsfjall marked the onset of a prolonged eruptive phase on the Reykjanes peninsula, with 11 subsequent eruptions occurring through to the time of writing, and continued volcanic unrest. Our findings demonstrate that even a relatively small volcanic event, such as the 2021 eruption, can lead to significant air pollution of SO$_2$ and PM. Due to its proximity to densely populated areas, the Fagradalsfjall eruption caused elevated pollutant concentrations, and air quality threshold exceedances comparable to those observed during the much larger Holuhraun eruption of 2014–2015. These results suggest that the Fagradalsfjall eruption generated sufficient air pollution that it may have triggered negative health responses, which should be investi-

gated retrospectively or during future events. Moreover, the high frequency of eruptions, and eruption-ignited wildfires in this region since 2021 raises the possibility of chronic exposure, which should also be examined, particularly given that the ongoing Reykjanes Fires eruptions may continue for several generations.

We showed that even the exceptionally dense, reference-grade air quality monitoring networks in the densely populated part of Iceland (Reykjavík capital and the Reykjanes peninsula) were insufficient to fully capture the fine-scale spatial variability of volcanic air pollution episodes. We recommend augmenting existing networks with well-calibrated low-cost sensors (LCS) to enhance spatial coverage, particularly in sensitive locations such as schools and hospitals, where vulnerable populations may be at greater risk. Previous studies on the Holuhraun eruption have demonstrated that public advisories on volcanic air pollution can serve as effective health protection measures. Therefore, improving the spatial resolution of air quality monitoring may further enhance public health outcomes by enabling more targeted and timely advice.

Understanding the volcanic air pollution in a uniquely Icelandic event like the Reykjanes Fires has important implications for how we manage and prepare for other eruptions globally. The fine-scale temporal and spatial variability in pollution dispersion identified in this study highlights the need for further investigation – not only in future Icelandic eruptions but also in other regions exposed to volcanic activity. Enhanced understanding of these dynamics can inform more effective monitoring strategies and public health responses worldwide.

Appendix A

Table A1. Variability in PM$_1$/PM$_{10}$ concentration ratios associated with different pollution sources in the Reykjavík capital area measured by three stations (G3-A, G3-D, G3-G). "Background": representative summer conditions; "2021" refers to eruption-period without volcanic plume influence; "Non-eruptive" covers summer periods in 2020 and 2022. "Volcanic plumes": periods during the 2021 eruption when the plume was advected toward Reykjavík (definitions of "fresh" and "mature" plumes in main text, Sect. 3.3). Data include one prolonged fresh plume event (> 24 h) and three discrete mature plume events, as mature plumes exhibit greater variability in PM size ratios. "Dust storms": two Icelandic highland desert storms (∼ 200 km source distance) affecting Reykjavík; "total" refers to the full duration of dust storm events with PM above background (PM$_{10}$ > 10 µg m^{-3}), while "peak" includes only hours with highly elevated PM (PM$_{10}$ > 50 µg m^{-3}). Station G3-G is listed first, as it is considered the most sensitive to the presence of volcanic plume due to its low background concentrations from local sources. Dates are in the format DD/MM/YYYY. n/a = not applicable.

	Start date	Start time	End date	End time	G3-G PM$_1$/PM$_{10}$	G3-A PM$_1$/PM$_{10}$	G3-D PM$_1$/PM$_{10}$	G3-G PM$_1$/PM$_{2.5}$	G3-A PM$_1$/PM$_{2.5}$	G3-D PM$_1$/PM$_{2.5}$	G3-G PM$_{2.5}$/PM$_{10}$	G3-A PM$_{2.5}$/PM$_{10}$	G3-D PM$_{2.5}$/PM$_{10}$
Background non-eruptive	1 May 2020	00:00	1 Sep 2020	00:00	0.16	0.15	0.13	0.44	0.43	0.22	0.35	0.34	0.61
Background 2021	1 Apr 2021	09:00	2 Apr 2021	10:00	0.17	0.19	0.24	0.41	0.43	0.45	0.42	0.43	0.54
Fresh plume	18 Jul 2021	10:00	19 Jul 2021	16:00	0.65	0.68	0.7	0.9	0.92	0.84	0.72	0.73	0.78
Mature plume 1	28 Apr 2021	08:00	29 Apr 2021	20:00	0.43	0.29	0.49	0.8	0.73	0.8	0.53	0.39	0.6
Mature plume 2	19 May 2021	14:00	21 May 2021	11:00	0.71	0.65	0.85	0.96	0.95	0.95	0.73	0.68	0.89
Mature plume 3	1 Jul 2021	09:00	6 Jul 2021	08:00	0.67	0.59	0.65	0.91	0.88	0.84	0.74	0.66	0.74
Desert dust 1 total	24 May 2021	20:00	29 May 2021	21:00	0.11	0.11	0.14	0.31	0.3	0.3	0.33	0.32	0.39
Desert dust 1 peak					0.05	0.05	0.04	0.18	0.17	0.17	0.26	0.26	0.27
Desert dust 2 total	3 Jun 2021	09:00	4 Jun 2021	11:00	0.12	0.25	0.17	0.33	0.44	0.31	0.31	0.42	0.42
Desert dust 2 peak					0.05	n/a	0.04	0.18	n/a	0.16	0.27	n/a	0.27

Figure A1. Lower-cost sensors used for the Fagradalsfjall 2021 eruption. Panel **(a)** shows the instrument installed in the field. The station was powered by a solar panel (triangular trellis at the back of the photo). The air intake was underneath the instrument (the white box at the front of the image). Panel **(b)** shows the air intake of the sensor. The air intake was designed in-house at the IMO taking into account local conditions, in particular the weather and dust resuspension. The cover was custom-made from Plexiglass with the sensors recessed behind it to be protected from dust, precipitation, and other potentially damaging environmental factors.
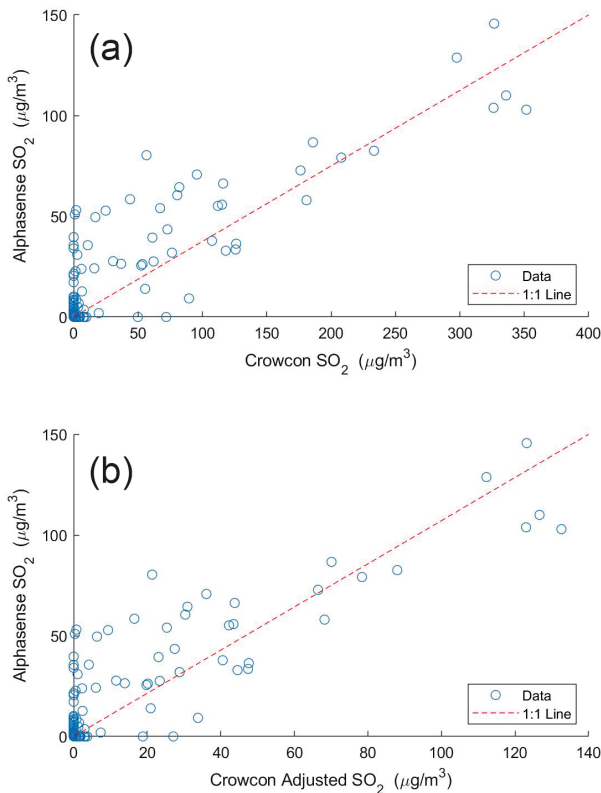
Figure A2. SO$_2$ concentrations measured by two types of lower-cost sensors (LCS) used in this study – Alphasense SO$_2$-B4 and Crowcon XGuard – during a field colocation at the eruption site (6–22 June 2021). Measurements from the two sensors showed a strong linear correlation ($r^2 = 0.70$), but Alphasense reported lower values relative to Crowcon, with a correlation coefficient of 0.38. **(a)** Correlation of raw data points from the two sensors. **(b)** Correlation after Crowcon data were adjusted using the correlation coefficient.
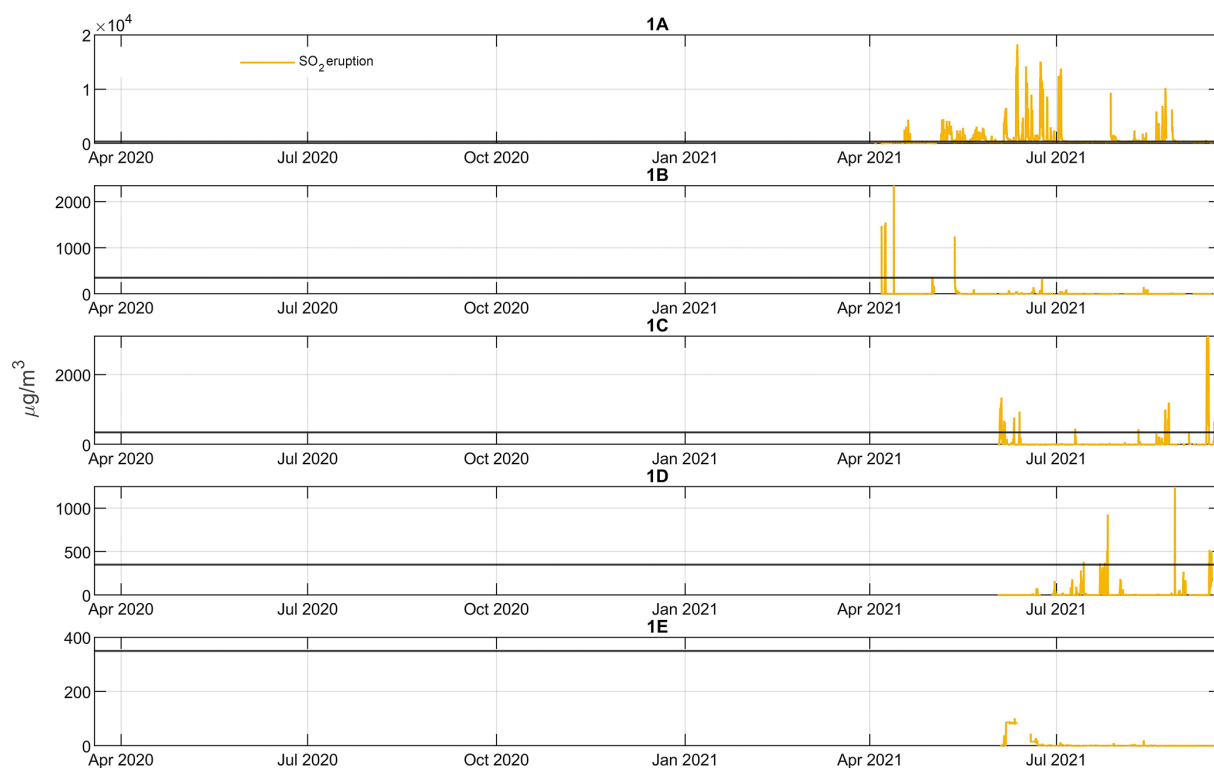
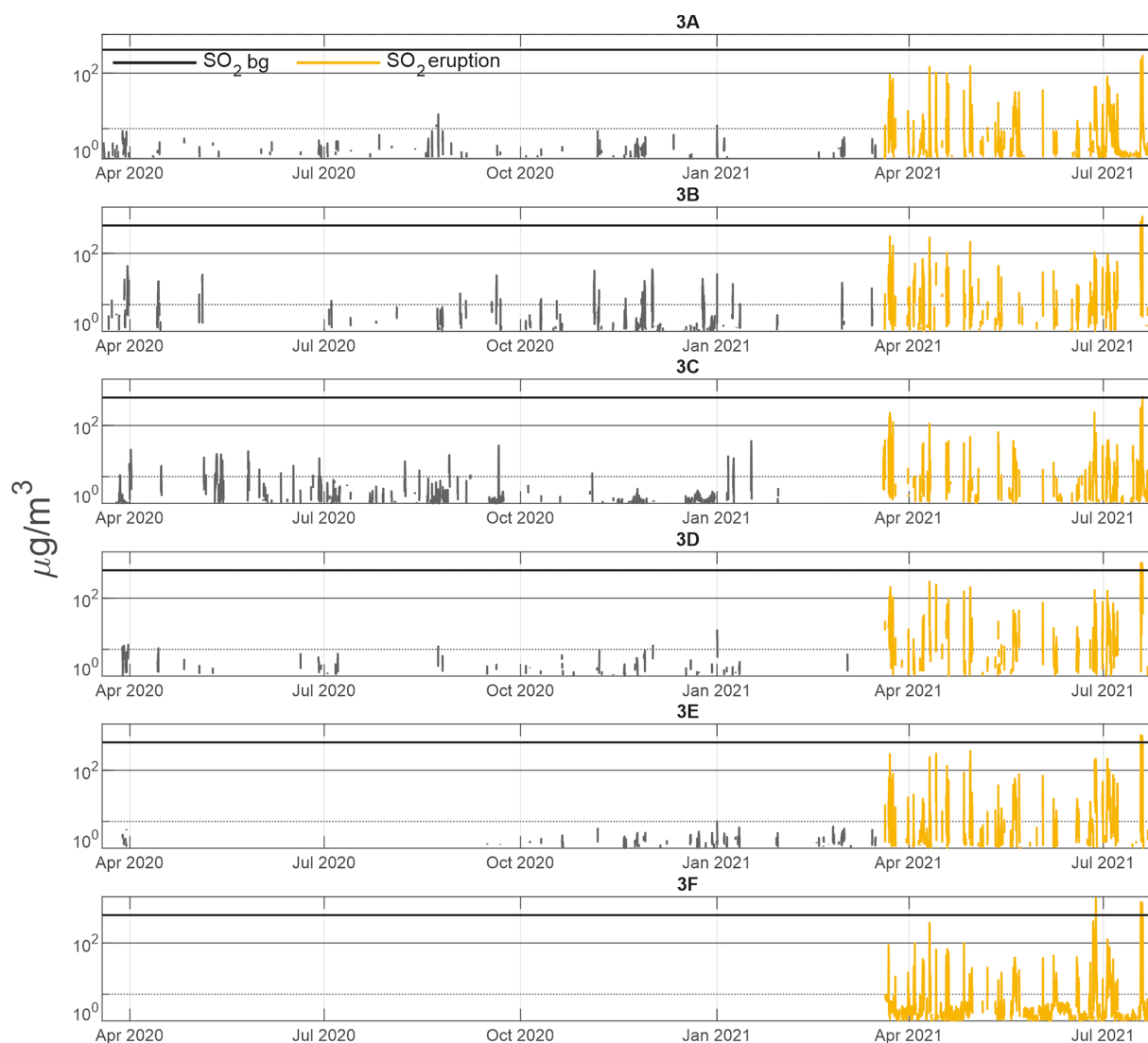**Figure A3.** Time series of hourly-mean concentrations SO$_2$ (μg m^{-3}), measured by the eruption site stations (G1 A–E) during the 2021 eruption. The stations were not in operation before the eruption and therefore there are no data on pre-eruptive background. The ID air quality threshold of 350 μg m^{-3} hourly-mean is shown on all panels with a black horizontal line. Note that the eruption-site LCS have low accuracy and were only used in this study to indicate time periods that were over the ID threshold, the absolute concentration values were not included in the analysis.
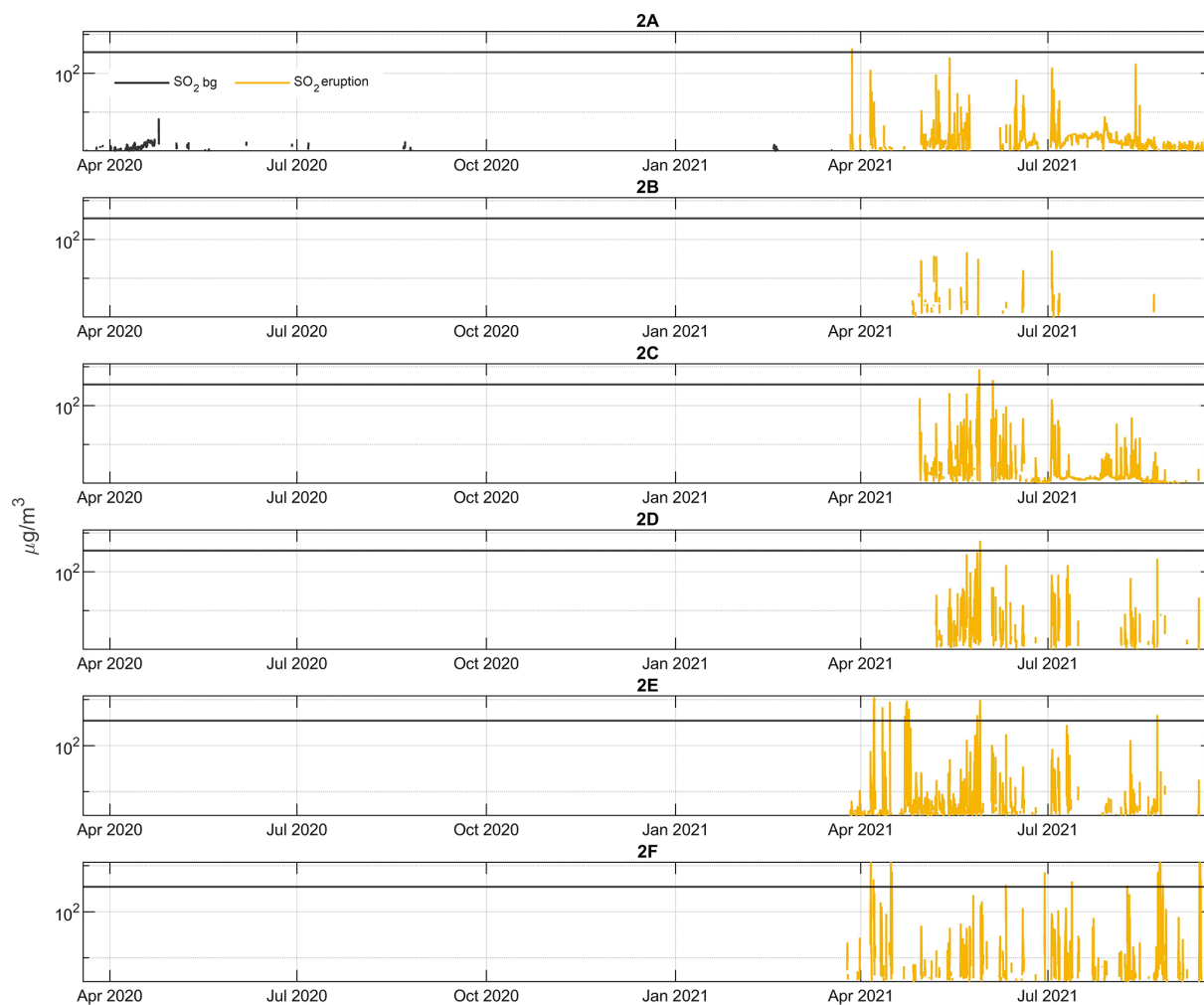
Figure A4. Time series of hourly-mean concentrations SO_2 ($\mu g\,m^{-3}$), measured by Reykjanes peninsula regulatory air quality stations (G2 A–F) during the 2021 eruption and the non-eruptive background in 2020 (bg). The ID air quality threshold of $350\,\mu g\,m^{-3}$ hourly-mean is shown on all panels with a black horizontal line. Please note the logarithmic y axis scale.
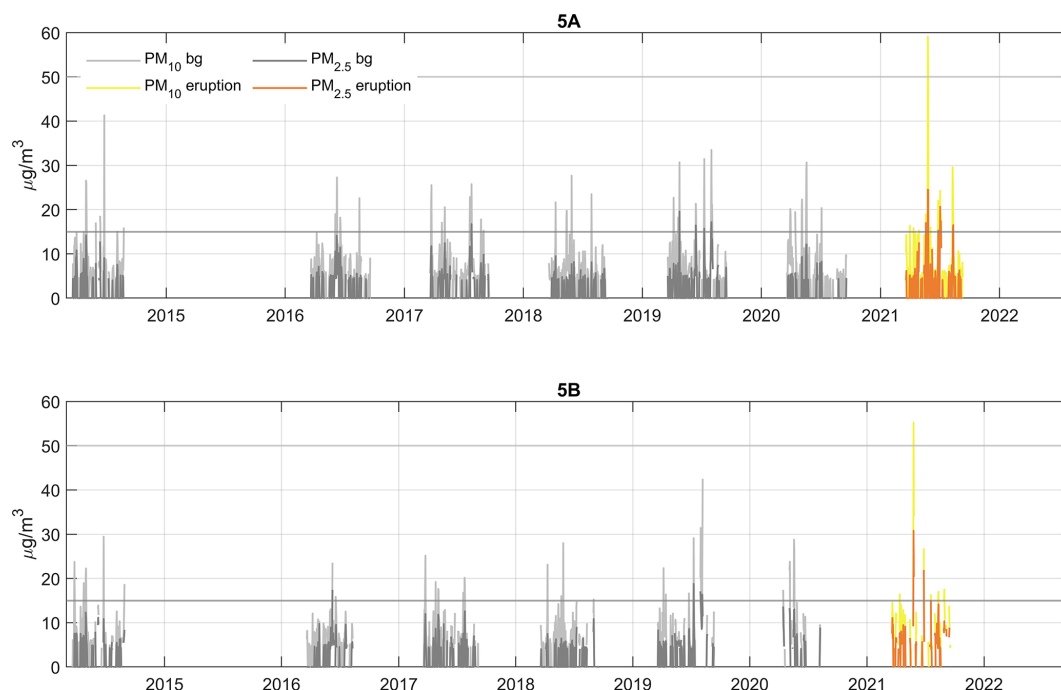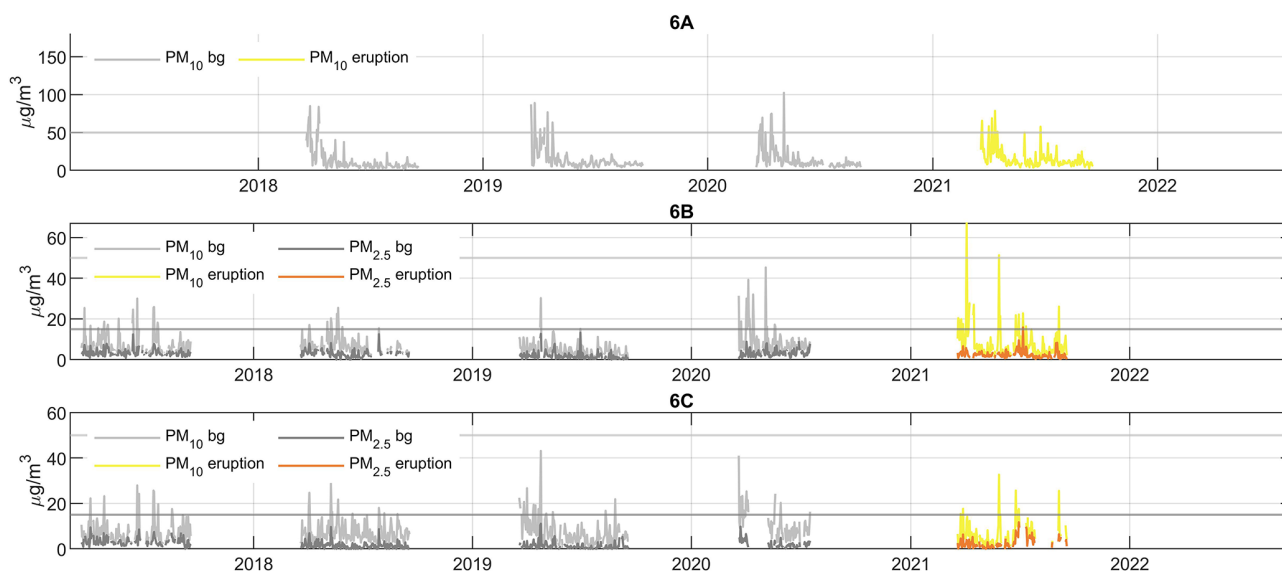
Figure A5. Time series of hourly-mean concentrations SO$_2$ (µg m^{-3}), measured by Reykjavík capital area regulatory air quality stations (G3 A–F) during the 2021 eruption and the non-eruptive background in 2020 (bg). The ID air quality threshold of 350 µg m^{-3} hourly-mean is shown on all panels with a black horizontal line. Please note the logarithmic y axis scale.
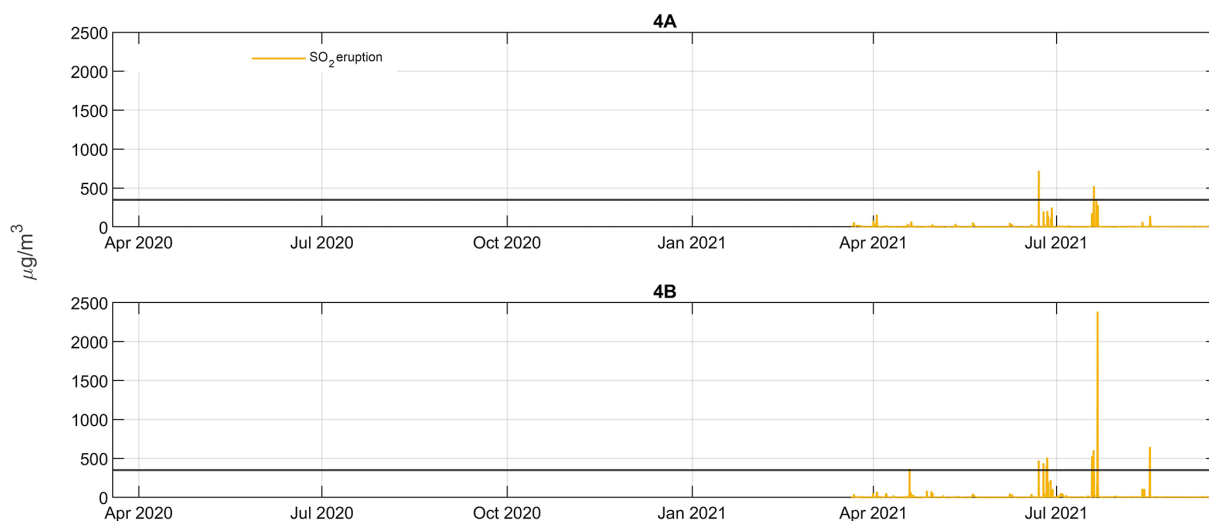
Figure A6. Time series of hourly-mean concentrations SO_2 ($\mu g\,m^{-3}$), measured in Southwest Iceland by regulatory air quality stations (G4 A and B) during the 2021 eruption. The stations were not in operation before the eruption and therefore there are no data on pre-eruptive background. The ID air quality threshold of $350\,\mu g\,m^{-3}$ hourly-mean is shown on all panels with a black horizontal line.
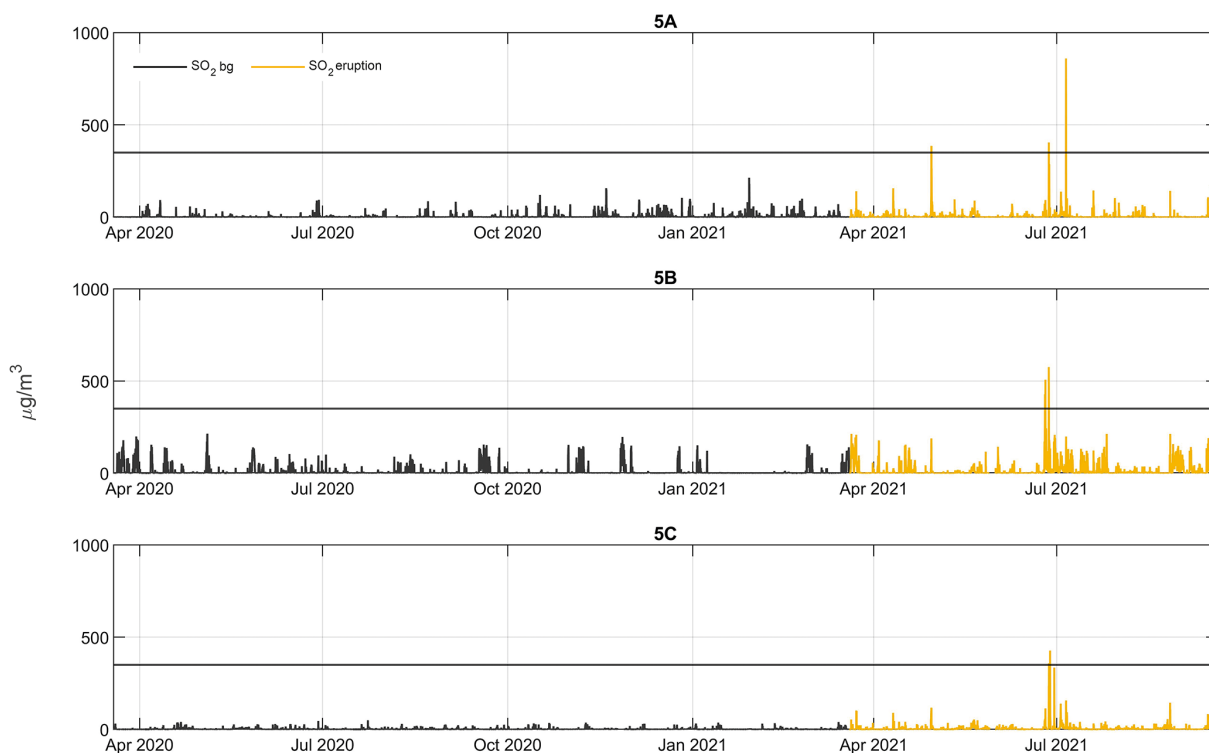
Figure A7. Time series of hourly-mean concentrations SO_2 ($\mu g\,m^{-3}$), measured in Hvalfjörður area by regulatory air quality stations (G5 A–C) during the 2021 eruption and the non-eruptive background in 2020 (bg). The ID air quality threshold of $350\,\mu g\,m^{-3}$ hourly-mean is shown on all panels with a black horizontal line.
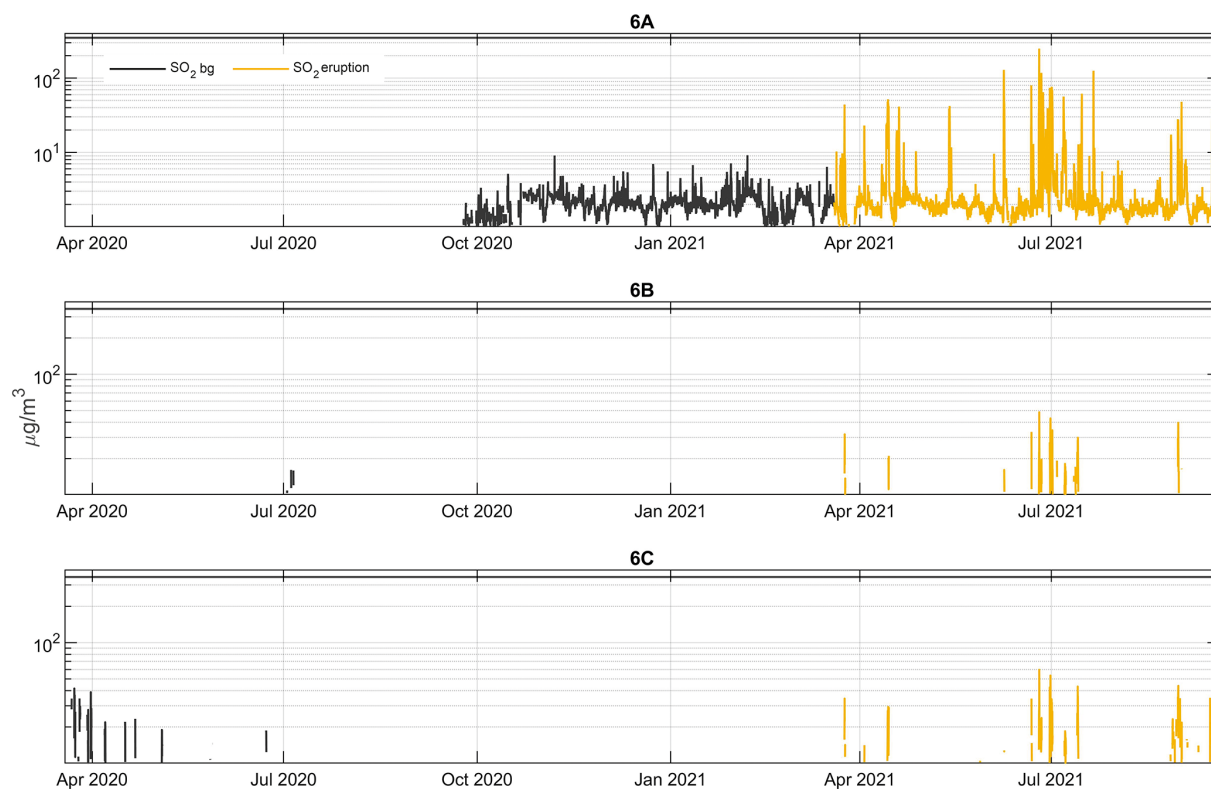
Figure A8. Time series of hourly-mean concentrations SO$_2$ (µg m^{-3}), measured in North Iceland by regulatory air quality stations (G6 A–C) during the 2021 eruption and the non-eruptive background in 2020 (bg). The ID air quality threshold of 350 µg m^{-3} hourly-mean is shown on all panels with a black horizontal line. Please note the logarithmic y axis scale.
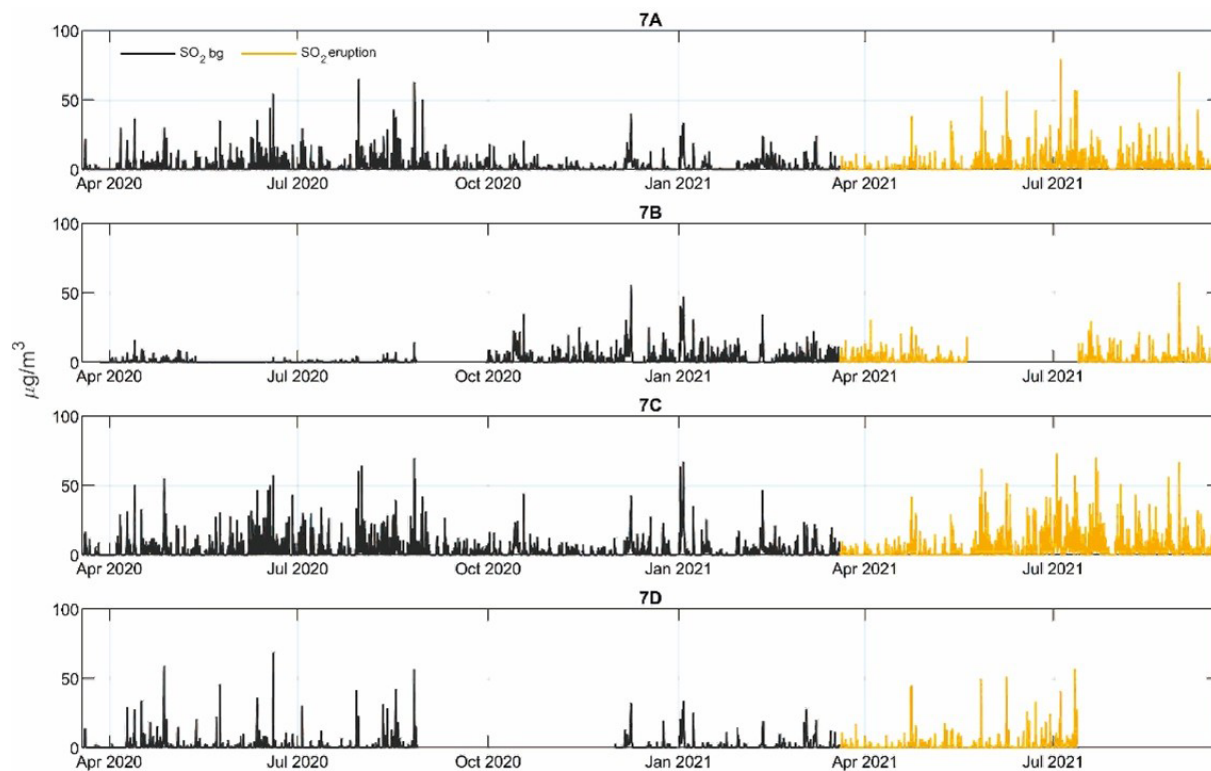
Figure A9. Time series of hourly-mean concentrations SO_2 ($\mu g\,m^{-3}$), measured in East Iceland by regulatory air quality stations (G7 A–D) during the 2021 eruption and the non-eruptive background in 2020 (bg). The ID air quality threshold of $350\,\mu g\,m^{-3}$ hourly-mean is shown on all panels with a black horizontal line.
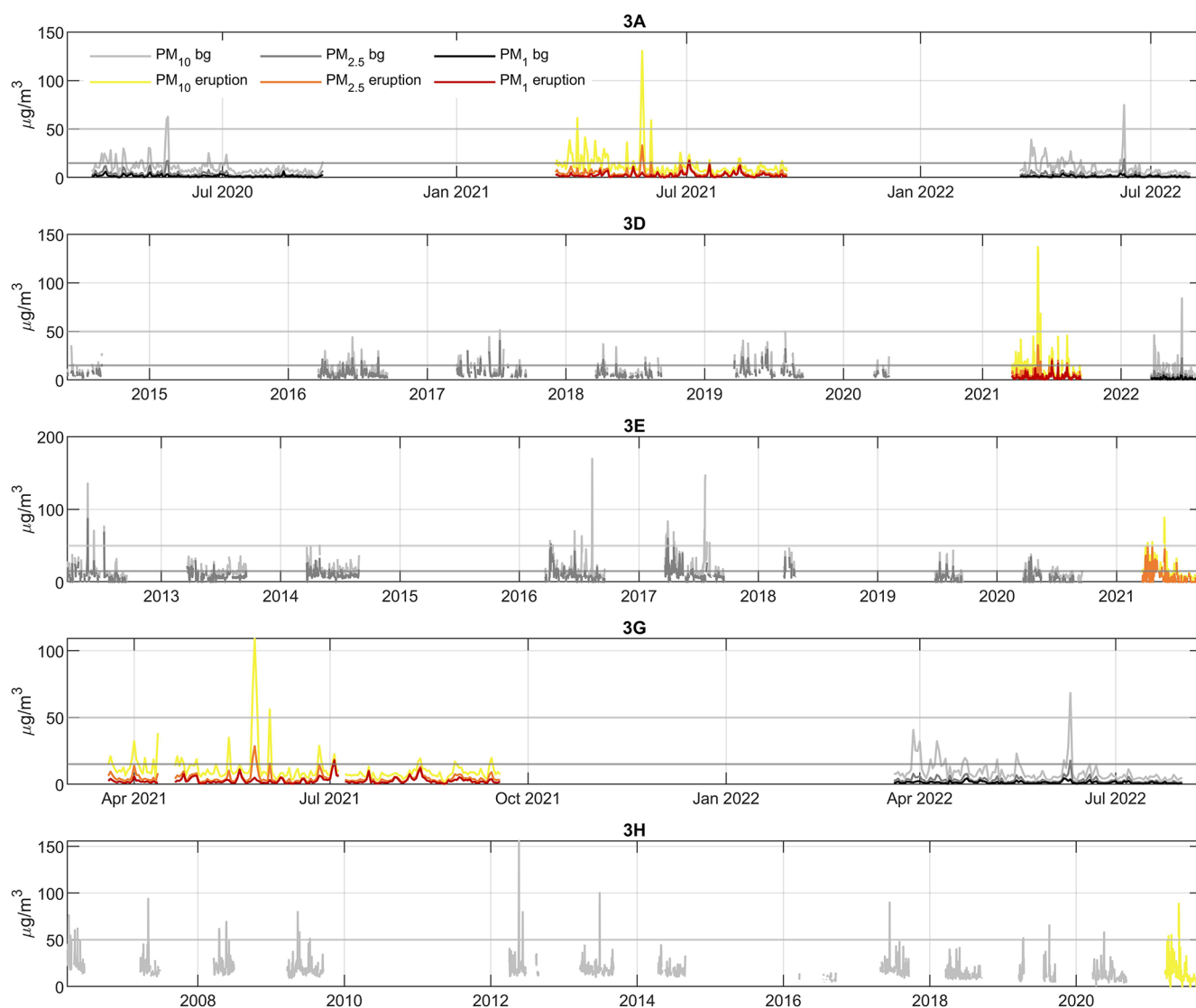
Figure A10. Time series of daily-mean concentrations of PM$_{10}$, PM$_{2.5}$ and PM$_1$ (µg m^{-3}) measured in Reykjavík capital area by regulatory air quality stations (G3 A, D, E, G, H) during the 2021 eruption and in the non-eruptive background (bg). The amount of non-eruptive background data varies between stations based on their installation date. The figures only include data for the period 19 March 20:00 UTC/local time–19 September 00:00 UTC/local time in each year, i.e. the period corresponding to the calendar dates and months of the 2021 eruption. See main text for the justification of this approach. The figures show the ID air quality thresholds for PM$_{10}$ and PM$_{2.5}$ of 50 and 15 µg m^{-3} daily-mean, respectively as grey horizontal lines. For PM$_1$, air quality thresholds have not been determined.

Figure A11. Time series of daily-mean concentrations of PM_{10}, and $PM_{2.5}$ ($\mu g\,m^{-3}$) measured in Hvalfjörður area by regulatory air quality stations (G5 A, B) during the 2021 eruption and in the non-eruptive background (bg). PM_1 was not measured at these stations. The amount of non-eruptive background data varies between stations based on their installation date. The figures only include data for the period 19 March 20:00 UTC/local time–19 September 00:00 UTC/local time in each year, i.e. the period corresponding to the calendar dates and months of the 2021 eruption. See main text for the justification of this approach. The figures show the ID air quality thresholds for PM_{10} and $PM_{2.5}$ of 50 and 15 $\mu g\,m^{-3}$ daily-mean, respectively as grey horizontal lines.

Figure A12. Time series of daily-mean concentrations of PM_{10}, and $PM_{2.5}$ ($\mu g\,m^{-3}$) measured in North Iceland by regulatory air quality stations (G6 A–C) during the 2021 eruption and in the non-eruptive background (bg). PM_1 was not measured at these stations. The figures only include data for the period 19 March 20:00 UTC/local time–19 September 00:00 UTC/local time in each year, i.e. the period corresponding to the calendar dates and months of the 2021 eruption. See main text for the justification of this approach. The figures show the ID air quality thresholds for PM_{10} and $PM_{2.5}$ of 50 and 15 $\mu g\,m^{-3}$ daily-mean, respectively as grey horizontal lines.
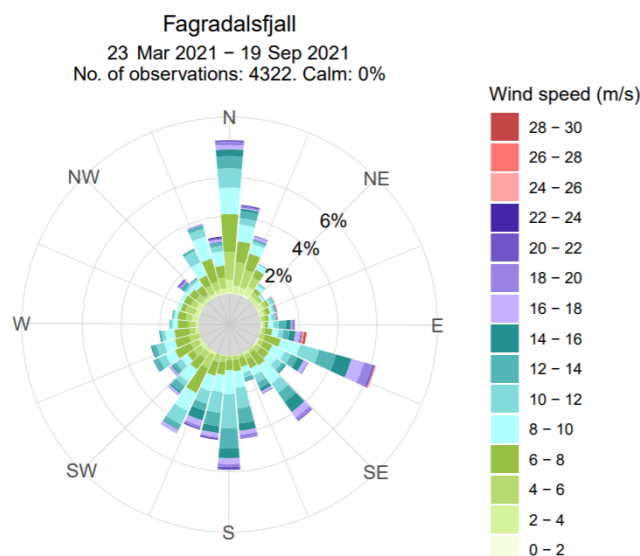
Figure A13. Wind rose shows wind direction (wind coming from) and wind speed measured by Icelandic Meteorological Office weather station at the Fagradalsfjall eruption site 23 March–19 September 2021.
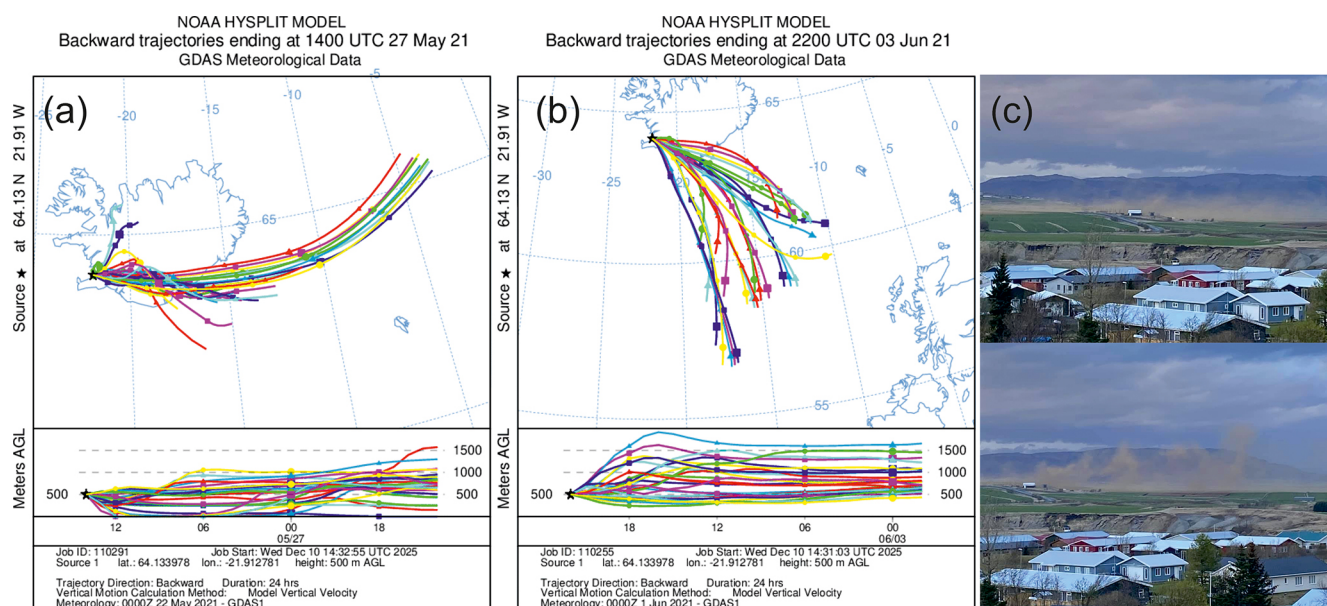
Figure A14. Evidence for two Icelandic highland storms affecting PM levels in Reykjavík capital area 24–29 May and 3–4 June 2021. **(a)** Ensemble back-trajectory analysis for the peak PM concentrations in Reykjavík on 27 May at 14:00 UTC/local time, calculated using the NOAA HYSPLIT model (Stein et al., 2015). **(b)** Ensemble back-trajectory analysis for the peak PM concentrations in Reykjavík on 3 June at 22:00 UTC/local time, calculated using the NOAA HYSPLIT model (Stein et al., 2015). The back-trajectory analysis for both events is consistent with well-known Icelandic dust storm source areas (Dagsson-Waldhauserova et al., 2014). **(c)** Two crowd-sourced photographs taken on 28 May 2021 near the source area identified by the back-trajectory analysis, confirming the dust storm origin. No photographs were available for the 3–4 June event. Photo credit: Sigurður H. Magnússon, posted on *Dust Storms in Iceland* Facebook page (28 May 2021).

References

Apte, J. S. and Manchanda, C.: High-resolution urban air pollution mapping, Science, 385, 380–385, https://doi.org/10.1126/science.adq3678, 2024.

Barsotti, S.: Probabilistic hazard maps for operational use: the case of SO$_2$ air pollution during the Holuhraun eruption (Bárðarbunga, Iceland) in 2014–2015, Bull. Volcanol., 82, 56, https://doi.org/10.1007/s00445-020-01395-3, 2020.

Barsotti, S., Parks, M. M., Pfeffer, M. A., Óladóttir, B. A., Barnie, T., Titos, M. M., Jónsdóttir, K., Pedersen, G. B. M., Hjartardóttir, Á. R., Stefansdóttir, G., Johannsson, T., Arason, Þ., Gudmundsson, M. T., Oddsson, B., Þrastarson, R. H., Ófeigsson, B. G., Vogfjörd, K., Geirsson, H., Hjörvar, T., von Löwis, S., Petersen, G. N., and Sigurðsson, E. M.: The eruption in Fagradalsfjall (2021, Iceland): how the operational monitoring and the volcanic hazard assessment contributed to its safe access, Nat. Hazards, 116, 3063–3092, https://doi.org/10.1007/s11069-022-05798-7, 2023.

Brauer, M., Roth, G. A., Aravkin, A. Y., et al.: Global burden and strength of evidence for 88 risk factors in 204 countries and 811 subnational locations, 1990–2021: a systematic analysis for the Global Burden of Disease Study 2021, Lancet, 403, 2162–2203, https://doi.org/10.1016/S0140-6736(24)00933-4, 2024.

Butwin, M. K., von Löwis, S., Pfeffer, M. A., and Thorsteinsson, T.: The effects of volcanic eruptions on the frequency of particulate matter suspension events in Iceland, J. Aerosol Sci., 128, 99–113, 2019.

Caplin, A., Ghandehari, M., Lim, C., Glimcher, P., and Thurston, G.: Advancing environmental exposure assessment science to benefit society, Nat. Commun., 10, 1236, https://doi.org/10.1038/s41467-019-09155-4, 2019.

Carlsen, H. K. and Thorsteinsson, T.: Associations between PM$_{10}$ from traffic, resuspension, sand storms and volcanic sources and asthma drugs dispensing, ResearchSquare, https://doi.org/10.21203/rs.3.rs-1017409/v1, 2021.

Carlsen, H. K., Ilyinskaya, E., Baxter, P. J., Schmidt, A., Thorsteinsson, T., Pfeffer, M. A., Barsotti, S., Dominici, F., Finnbjornsdottir, R. G., Jóhannsson, T., Aspelund, T., Gislason, T., Valdimarsdóttir, U., Briem, H., and Gudnason, T.: Increased respiratory morbidity associated with exposure to a mature volcanic plume from a large Icelandic fissure eruption, Nat. Commun., 12, 2161, https://doi.org/10.1038/s41467-021-22432-5, 2021a.

Carlsen, H. K., Valdimarsdóttir, U., Briem, H., Dominici, F., Finnbjornsdottir, R. G., Jóhannsson, T., Aspelund, T., Gislason, T., and Gudnason, T.: Severe volcanic SO$_2$ exposure and respiratory morbidity in the Icelandic population–a register study, Environ. Health, 20, 1–12, 2021b.

Crawford, B., Hagan, D. H., Grossman, I., Cole, E., Holland, L., Heald, C. L., and Kroll, J. H.: Mapping pollution exposure and chemistry during an extreme air quality event (the 2018 Kīlauea eruption) using a low-cost sensor network, P. Natl. Acad. Sci. USA, 118, e2025540118, https://doi.org/10.1073/pnas.2025540118, 2021.

Crilley, L. R., Shaw, M., Pound, R., Kramer, L. J., Price, R., Young, S., Lewis, A. C., and Pope, F. D.: Evaluation of a low-cost optical particle counter (Alphasense OPC-N2) for ambient air monitoring, Atmos. Meas. Tech., 11, 709–720, https://doi.org/10.5194/amt-11-709-2018, 2018.

Dagsson-Waldhauserova, P., Arnalds, O., and Olafsson, H.: Long-term variability of dust events in Iceland (1949–2011), Atmos. Chem. Phys., 14, 13411–13422, https://doi.org/10.5194/acp-14-13411-2014, 2014.

Dagsson-Waldhauserova, P., Magnusdottir, A. Ö., Olafsson, H., and Arnalds, O.: The Spatial Variation of Dust Particulate Matter Concentrations during Two Icelandic Dust Storms in 2015, Atmosphere, 7, 77, https://doi.org/10.3390/atmos7060077, 2016.

Felton, D., Grange, G., Damby, D., Bronstein, A., and Spyker, D.: Sulfur dioxide monitoring associated with the 2018 Kilauea Lower East Rift Zone Eruption, in: International Union of Toxicology (IUTOX) 15th International Congress of Toxicology, Honolulu, HI, USA, 2019.

Freire, S., Florczyk, A. J., Pesaresi, M., and Sliuzas, R.: An Improved Global Analysis of Population Distribution in Proximity to Active Volcanoes, 1975–2015, ISPRS Int. J. Geo-Inf., 8, 341, https://doi.org/10.3390/ijgi8080341, 2019.

Gan, T., Chu, J., Bambrick, H., Guo, X., and Hu, W.: Long-term exposure to PM$_1$ and liver cancer mortality: Insights into the role of smaller particulate fractions, Ecotoxicol. Environ. Safe., 300, 118467, https://doi.org/10.1016/j.ecoenv.2025.118467, 2025.

Gíslason, S. R., Stefánsdóttir, G., Pfeffer, M. A., Barsotti, S., Jóhannsson, Th., Galeczka, I., Bali, E., Sigmarsson, O., Stefánsson, A., Keller, N. S., Sigurdsson, á., Bergsson, B., Galle, B., Jacobo, V. C., Arellano, S., Aiuppa, A., Jónasdóttir, E. B., Eiríksdóttir, E. S., Jakobsson, S., Guðfinnsson, G. H., Halldórsson, S. A., Gunnarsson, H., Haddadi, B., Jónsdóttir, I., Thordarson, Th., Riishuus, M., Högnadóttir, Th., Dürig, T., Pedersen, G. B. M., Höskuldsson, Á., and Gudmundsson, M. T.: Environmental pressure from the 2014–15 eruption of Bárðarbunga volcano, Iceland, Geochem. Perspect. Lett., 84–93, https://doi.org/10.7185/geochemlet.1509, 2015.

Grattan, J.: The distal impact of Icelandic volcanic gases and aerosols in Europe: a review of the 1783 Laki Fissure eruption and environmental vulnerability in the late 20th century, Geol. Soc. Lond. Eng. Geol. Spec. Publ., 15, 97–103, https://doi.org/10.1144/GSL.ENG.1998.015.01.10, 1998.

Green, J. R., Fiddler, M. N., Holloway, J. S., Fibiger, D. L., McDuffie, E. E., Campuzano-Jost, P., Schroder, J. C., Jimenez, J. L., Weinheimer, A. J., Aquino, J., Montzka, D. D., Hall, S. R., Ullmann, K., Shah, V., Jaeglé, L., Thornton, J. A., Bililign, S., and Brown, S. S.: Rates of wintertime atmospheric SO$_2$ oxidation based on aircraft observations during clear-sky conditions over the eastern United States, J. Geophys. Res.-Atmos., 124, 6630–6649, 2019.

Guo, H., Li, X., Wei, J., Li, W., Wu, J., and Zhang, Y.: Smaller particular matter, larger risk of female lung cancer incidence? Evi-

dence from 436 Chinese counties, BMC Publ. Health, 22, 344, https://doi.org/10.1186/s12889-022-12622-1, 2022.

Heaviside, C., Witham, C., and Vardoulakis, S.: Potential health impacts from sulphur dioxide and sulphate exposure in the UK resulting from an Icelandic effusive volcanic eruption, Sci. Total Environ., 145549, https://doi.org/10.1016/j.scitotenv.2021.145549, 2021.

Horwell, C. J., Elias, T., Covey, J., Bhandari, R., and Truby, J.: Perceptions of volcanic air pollution and exposure reduction practices on the Island of Hawai'i: Working towards socially relevant risk communication, Int. J. Disast. Risk Reduct., 95, 103853, https://doi.org/10.1016/j.ijdrr.2023.103853, 2023.

Icelandic Directive: Reglugerð um brennisteinsdíoxíð, köfnunarefnisdíoxíð og köfnunarefnisoxíð, bensen, kolsýring, svifryk og blý í andrúmsloftinu, B-Deild, Nr. 920, https://island.is/reglugerdir/nr/0920-2016 (last access: 21 December 2025), 2016.

Icelandic Meteorological office: Hazard map, https://en.vedur.is/volcanoes/fagradalsfjall-eruption/hazard-map/ (last access: 14 December 2025), 2025.

Ilyinskaya, E., Martin, R. S., and Oppenheimer, C.: Aerosol formation in basaltic lava fountaining: Eyjafjallajökull volcano, Iceland, J. Geophys. Res., 117, D00U27, https://doi.org/10.1029/2011JD016811, 2012.

Ilyinskaya, E., Schmidt, A., Mather, T. A., Pope, F. D., Witham, C., Baxter, P., Jóhannsson, T., Pfeffer, M., Barsotti, S., Singh, A., Sanderson, P., Bergsson, B., McCormick Kilbride, B., Donovan, A., Peters, N., Oppenheimer, C., and Edmonds, M.: Understanding the environmental impacts of large fissure eruptions: Aerosol and gas emissions from the 2014–2015 Holuhraun eruption (Iceland), Earth Planet. Sc. Lett., 472, 309–322, https://doi.org/10.1016/j.epsl.2017.05.025 2017.

Ilyinskaya, E., Mason, E., Wieser, P. E., Holland, L., Liu, E. J., Mather, T. A., Edmonds, M., Whitty, R. C. W., Elias, T., Nadeau, P. A., Schneider, D., McQuaid, J. B., Allen, S. E., Harvey, J., Oppenheimer, C., Kern, C., and Damby, D.: Rapid metal pollutant deposition from the volcanic plume of Kīlauea, Hawai'i, Commun. Earth Environ., 2, 1–15, https://doi.org/10.1038/s43247-021-00146-2, 2021.

Ilyinskaya, E., Snæbjarnarson, V., Carlsen, H. K., and Oddsson, B.: Brief communication: Small-scale geohazards cause significant and highly variable impacts on emotions, Nat. Hazards Earth Syst. Sci., 24, 3115–3128, https://doi.org/10.5194/nhess-24-3115-2024, 2024.

Janssen, N. A. H., Fischer, P., Marra, M., Ameling, C., and Cassee, F. R.: Short-term effects of PM$_{2.5}$, PM$_{10}$ and PM$_{2.5-10}$ on daily mortality in the Netherlands, Sci. Total Environ., 463–464, 20–26, https://doi.org/10.1016/j.scitotenv.2013.05.062, 2013.

Longo, B. M.: The Kilauea Volcano Adult Health Study, Nurs. Res., 58, https://doi.org/10.1097/NNR.0b013e3181900cc5, 2009.

Longo, B. M., Rossignol, A., and Green, J. B.: Cardiorespiratory health effects associated with sulphurous volcanic air pollution, Publ. Health, 122, 809–820, https://doi.org/10.1016/j.puhe.2007.09.017, 2008.

Martin, R. S., Ilyinskaya, E., Sawyer, G. M., Tsanev, V. I., and Oppenheimer, C.: A re-assessment of aerosol size distributions from Masaya volcano (Nicaragua), Atmos. Environ., 45, 547–560, https://doi.org/10.1016/j.atmosenv.2010.10.049, 2011.

Mason, E., Wieser, P. E., Liu, E. J., Edmonds, M., Ilyinskaya, E., Whitty, R. C. W., Mather, T. A., Nadeau, P. A., Wilkes, T. C., McGonigle, A. J. S., Pering, T. D., Mims, F. M., Kern, C., Schneider, D. J., and Oppenheimer, C.: Volatile metal emissions from volcanic degassing and lava–seawater interactions at Kīlauea Volcano, Hawai'i, Commun. Earth Environ., 2, 1–16, https://doi.org/10.1038/s43247-021-00145-3, 2021.

Mather, T. A., Pyle, D. M., and Oppenheimer, C.: Tropospheric volcanic aerosol, in: Geophysical Monograph Series, vol. 139, edited by: Robock, A. and Oppenheimer, C., American Geophysical Union, Washington, D.C., 189–212, https://doi.org/10.1029/139GM12, 2003.

Mcdonnell, W. F., Nishino-Ishikawa, N., Petersen, F. F., Chen, L. H., and Abbey, D. E.: Relationships of mortality with the fine and coarse fractions of long-term ambient PM$_{10}$ concentrations in nonsmokers, J. Exp. Sci. Environ. Epidemiol., 10, 427–436, https://doi.org/10.1038/sj.jea.7500095, 2000.

Nakashima, M. and Dagsson-Waldhauserová, P.: A 60 Year Examination of Dust Day Activity and Its Contributing Factors From Ten Icelandic Weather Stations From 1950 to 2009, Front. Earth Sci., 6, https://doi.org/10.3389/feart.2018.00245, 2019.

Pattantyus, A. K., Businger, S., and Howell, S. G.: Review of sulfur dioxide to sulfate aerosol chemistry at Kīlauea Volcano, Hawai'i, Atmos. Environ., 185, 262–271, https://doi.org/10.1016/j.atmosenv.2018.04.055, 2018.

Pfeffer, M. A., Arellano, S., Barsotti, S., Petersen, G. N., Barnie, T., Ilyinskaya, E., Hjörvar, T., Bali, E., Pedersen, G. B. M., Guðmundsson, G. B., Vogfjörð, K., Ranta, E. J., Óladóttir, B. A., Edwards, B. A., Moussallam, Y., Stefánsson, A., Scott, S. W., Smekens, J.-F., Varnam, M., and Titos, M.: SO$_2$ emission rates and incorporation into the air pollution dispersion forecast during the 2021 eruption of Fagradalsfjall, Iceland, J. Volcanol. Geoth. Res., 449, 108064, https://doi.org/10.1016/j.jvolgeores.2024.108064, 2024.

Schmidt, A., Ostro, B., Carslaw, K. S., Wilson, M., Thordarson, T., Mann, G. W., and Simmons, A. J.: Excess mortality in Europe following a future Laki-style Icelandic eruption, P. Natl. Acad. Sci. USA, 108, 15710–15715, https://doi.org/10.1073/pnas.1108569108, 2011.

Schmidt, A., Leadbetter, S., Theys, N., Carboni, E., Witham, C. S., Stevenson, J. A., Birch, C. E., Thordarson, T., Turnock, S., Barsotti, S., Delaney, L., Feng, W., Grainger, R. G., Hort, M. C., Höskuldsson, Á., Ialongo, I., Ilyinskaya, E., Jóhannsson, T., Kenny, P., Mather, T. A., Richards, N. A. D., and Shepherd, J.: Satellite detection, long-range transport and air quality impacts of volcanic sulfur dioxide from the 2014–15 flood lava eruption at Bárðarbunga (Iceland), J. Geophys. Res.-Atmos., 2015JD023638, https://doi.org/10.1002/2015JD023638, 2015.

Sigurgeirsson, M. and Einarsson, S.: Reykjanes and Svartsengi volcanic systems, in: Catalogue of Icelandic Volcanoes, IMO, UI and CPD-NCIP, http://icelandicvolcanoes.is/?volcano=REY (last access: 21 December 2025), 2019.

Sokhi, R. S., Moussiopoulos, N., Baklanov, A., Bartzis, J., Coll, I., Finardi, S., Friedrich, R., Geels, C., Grönholm, T., Halenka, T., Ketzel, M., Maragkidou, A., Matthias, V., Moldanova, J., Ntziachristos, L., Schäfer, K., Suppan, P., Tsegas, G., Carmichael, G., Franco, V., Hanna, S., Jalkanen, J.-P., Velders, G. J. M., and Kukkonen, J.: Advances in air quality research – current and emerging challenges, Atmos. Chem. Phys., 22, 4615–4703, https://doi.org/10.5194/acp-22-4615-2022, 2022.

Sonnek, K. M., Mårtensson, T., Veibäck, E., Tunved, P., Grahn, H., von Schoenberg, P., Brännström, N., and Bucht, A.: The impacts of a Laki-like eruption on the present Swedish society, Nat. Hazards, 88, 1565–1590, https://doi.org/10.1007/s11069-017-2933-0, 2017.

Statistics Iceland: Average annual population by municipality, age and sex 1998–2022 – Current municipalities, https://px.hagstofa.is/pxen/pxweb/en/Ibuar/Ibuar__mannfjoldi__2_byggdir__sveitarfelog/MAN02008.px (last access: 21 December 2025), 2022.

Stein, A. F., Draxler, R. R., Rolph, G. D., Stunder, B. J. B., Cohen, M. D., and Ngan, F.: NOAA's HYSPLIT Atmospheric Transport and Dispersion Modeling System, B. Am. Meteorol. Soc., 96, 2059–2077, https://doi.org/10.1175/BAMS-D-14-00110.1, 2015.

Stewart, C., Damby, D. E., Horwell, C. J., Elias, T., Ilyinskaya, E., Tomašek, I., Longo, B. M., Schmidt, A., Carlsen, H. K., Mason, E., Baxter, P. J., Cronin, S., and Witham, C.: Volcanic air pollution and human health: recent advances and future directions, Bull. Volcanol., 84, 11, https://doi.org/10.1007/s00445-021-01513-9, 2021.

Tam, E., Miike, R., Labrenz, S., Sutton, A. J., Elias, T., Davis, J., Chen, Y.-L., Tantisira, K., Dockery, D., and Avol, E.: Volcanic air pollution over the Island of Hawai'i: Emissions, dispersal, and composition. Association with respiratory symptoms and lung function in Hawai'i Island school children, Environ. Int., 92–93, 543–552, https://doi.org/10.1016/j.envint.2016.03.025, 2016.

Tomášková, H., Šlachtová, H., Tomášek, I., Polaufová, P., Hellebrandová, L., Šplíchalová, A., and Argalášová, L': Short-term Exposure to PM$_1$ and Total and Specific Mortality in the Czech Republic, in: Recent Advances in Environmental Science from the Euro-Mediterranean and Surrounding Regions 4th Edn., Springer, Cham, 1107–1110, https://doi.org/10.1007/978-3-031-51904-8_241, 2024.

Trigo, R. M., Vaquero, J. M., and Stothers, R. B.: Witnessing the impact of the 1783–1784 Laki eruption in the Southern Hemisphere, Climatic Change, 99, 535–546, hhttps://doi.org/10.1007/s10584-009-9676-1, 2009.

Twigg, M. M., Ilyinskaya, E., Beccaceci, S., Green, D. C., Jones, M. R., Langford, B., Leeson, S. R., Lingard, J. J. N., Pereira, G. M., Carter, H., Poskitt, J., Richter, A., Ritchie, S., Simmons, I., Smith, R. I., Tang, Y. S., Van Dijk, N., Vincent, K., Nemitz, E., Vieno, M., and Braban, C. F.: Impacts of the 2014–2015 Holuhraun eruption on the UK atmosphere, Atmos. Chem. Phys., 16, 11415–11431, https://doi.org/10.5194/acp-16-11415-2016, 2016.

UKCEH: Atmospheric sulphur dioxide levels hit historic high in Scotland following Icelandic volcanic eruption, UK Centre for Ecology & Hydrology, https://www.ceh.ac.uk/press/atmospheric-sulphur-dioxide-levels-hit-historic-high-scotland (last access: 21 December 2025), 2024.

U.S. EPA: Integrated Science Assessment (ISA) for Sulfur Oxides – Health Criteria (Final Report, Sep 2008), U.S. Environmental Protection Agency, Washington, DC, EPA/600/R-08/047F, https://assessments.epa.gov/isa/document/&deid=198843 (last access: 21 December 2025), 2008.

Whitty, R., Pfeffer, M., Ilyinskaya, E., Roberts, T., Schmidt, A., Barsotti, S., Strauch, W., Crilley, L., Pope, F., Bellanger, H., Mendoza, E., Mather, T., Liu, E., Peters, N., Taylor, I., Francis, H., Leiva, X. H., Lynch, D., Nobert, S., and Baxter, P.: Effectiveness of low-cost air quality monitors for identifying volcanic SO$_2$ and PM downwind from Masaya volcano, Nicaragua, Volcanica, 5, 33–59, https://doi.org/10.30909/vol.05.01.3359, 2022.

Whitty, R. C. W., Ilyinskaya, E., Mason, E., Wieser, P. E., Liu, E. J., Schmidt, A., Roberts, T., Pfeffer, M. A., Brooks, B., Mather, T. A., Edmonds, M., Elias, T., Schneider, D. J., Oppenheimer, C., Dybwad, A., Nadeau, P. A., and Kern, C.: Spatial and Temporal Variations in SO$_2$ and PM$_{2.5}$ Levels Around Kīlauea Volcano, Hawai'i During 2007–2018, Front. Earth Sci., 8, https://doi.org/10.3389/feart.2020.00036, 2020.

World Health Organization: WHO global air quality guidelines: particulate matter (PM$_{2.5}$ and PM$_{10}$), ozone, nitrogen dioxide, sulfur dioxide and carbon monoxide, xxi, World Health Organization, 267 pp., ISBN 9789240034228, https://www.who.int/publications/i/item/9789240034228 (last access: 21 December 2025), 2021.

Yang, M., Chu, C., Bloom, M. S., Li, S., Chen, G., Heinrich, J., Markevych, I., Knibbs, L. D., Bowatte, G., Dharmage, S. C., Komppula, M., Leskinen, A., Hirvonen, M.-R., Roponen, M., Jalava, P., Wang, S.-Q., Lin, S., Zeng, X.-W., Hu, L.-W., Liu, K.-K., Yang, B.-Y., Chen, W., Guo, Y., and Dong, G.-H.: Is smaller worse? New insights about associations of PM$_1$ and respiratory health in children and adolescents, Environ. Int., 120, 516–524, 2018.

Zhang, Y., Ding, Z., Xiang, Q., Wang, W., Huang, L., and Mao, F.: Short-term effects of ambient PM$_1$ and PM$_{2.5}$ air pollution on hospital admission for respiratory diseases: Case-crossover evidence from Shenzhen, China, Int. J. Hyg. Environ. Health, 224, 113418, https://doi.org/10.1016/j.ijheh.2019.11.001, 2020.